Regulation of Ribosome Biogenesis by Nucleostemin 3 Promotes Local and Systemic Growth in *Drosophila*

Tom A. Hartl,*[,1] Julie Ni,*[,1] Jian Cao,* Kaye L. Suyama,* Stephanie Patchett,[†] Cyril Bussiere,[‡] Dan Yi Gui,* Sheng Tang,* Daniel D. Kaplan,*[,2] Matthew Fish,* Arlen W. Johnson,[†] and Matthew P. Scott*[,3]

*Departments of Developmental Biology, Genetics, and Bioengineering, Howard Hughes Medical Institute, Stanford University School of Medicine, Stanford, California 94305, [†]Section of Molecular Genetics and Microbiology and the Institute for Cell and Molecular Biology, University of Texas, Austin, Texas 78712, and [‡]School of Medicine, Texas Tech University Health Sciences Center, Lubbock, Texas 79415

ABSTRACT Nucleostemin 3 (NS3) is an evolutionarily conserved protein with profound roles in cell growth and viability. Here we analyze cell-autonomous and non-cell-autonomous growth control roles of NS3 in *Drosophila* and demonstrate its GTPase activity using genetic and biochemical assays. Two null alleles of *ns3*, and RNAi, demonstrate the necessity of NS3 for cell autonomous growth. A hypomorphic allele highlights the hypersensitivity of neurons to lowered NS3 function. We propose that NS3 is the functional ortholog of yeast and human Lsg1, which promotes release of the nuclear export adapter from the large ribosomal subunit. Release of the adapter and its recycling to the nucleus are essential for sustained production of ribosomes. The ribosome biogenesis role of NS3 is essential for proper rates of translation in all tissues and is necessary for functions of growth-promoting neurons.

THE rate and fidelity of protein synthesis in a cell depend upon the proper assembly of the ribosome. Ribosome biogenesis begins in the nucleolus with the synthesis of ribosomal RNA (rRNA) and culminates in the creation of a fully functional ribosome competent to initiate protein synthesis in the cytoplasm. This process is impressively intricate, requiring ~200 factors acting at various levels. Major ribosome biogenesis steps include directing rRNA post-transcriptional modification, 90S cleavage, folding/assembly of the small (40S) and large (60S) ribosomal subunits, and proper transport from the nucleus to cytoplasm where final maturation occurs (Zemp and Kutay 2007; Henras *et al.* 2008; Staley and Woolford 2009; Strunk and Karbstein 2009; Panse and Johnson 2010).

Export of pre-ribosomal subunits from the nucleus to the cytoplasm requires movement through the nuclear pore complex (Hurt *et al.* 1999; Moy and Silver 1999; Stage-Zimmermann *et al.* 2000; Seiser *et al.* 2006). The pre-60S subunit achieves nuclear export by recruiting nuclear export factors, including the nuclear export signal (NES)-bearing protein Nmd3 (Ho *et al.* 2000; Gadal *et al.* 2001). Equally essential is recycling of Nmd3 from the cytoplasm back to the nucleus for subsequent rounds of pre-60S export. The release of Nmd3 appears to be the last step of a highly ordered pathway of ribosome maturation in the cytoplasm (Lo *et al.* 2010). Studies in *Saccharomyces cerevisiae* implicated RpL10p and Lsg1p as factors critical for Nmd3 recycling. Loss of either RpL10p or Lsg1p caused accumulation of Nmd3 in the cytoplasm, which precluded its ability to return to the nucleus for additional rounds of pre-60S export (Hedges *et al.* 2005). Thus, the loss of Nmd3p, RpL10p, or Lsg1p through mutation causes 60S subunit deficiency in the cytoplasm.

In *Drosophila*, a well-known class of mutations, called *Minutes* affects ribosome assembly. *Minutes* have delayed development and small or "minute" bristles; mutations affecting 66 of the 88 predicted ribosomal proteins have this phenotype (Marygold *et al.* 2007). The first *Minute* gene was discovered by Calvin Bridges and T. H. Morgan in 1919 (Bridges and Morgan 1923). This allele of *RpS8* was the

doi: 10.1534/genetics.112.149104
Manuscript received December 26, 2012; accepted for publication January 30, 2013
Supporting information is available online at http://www.genetics.org/lookup/suppl/doi:10.1534/genetics.112.149104/-/DC1.
[1]These authors contributed equally to this work.
[2]Present address: NGM Biopharmaceuticals, Inc., 630 Gateway Blvd., South San Francisco, CA 94080.
[3]Corresponding author: Clark Center, West Wing W252, 318 Campus Dr., Stanford University School of Medicine, Stanford, CA 94305. E-mail: mscott@stanford.edu

founding member of what came to be a large class of genes that are often haplo-insufficient. Later, with the advent of molecular biology, it became clear that most *Minute* genes code for ribosomal proteins. The conclusion was that the normal rate of progression through larval development and normal bristle synthesis are highly sensitive to protein synthesis rates (Lambertsson 1998).

Loss-of-function alleles for different ribosomal protein genes can have distinctive phenotypes in addition to the shared classical *Minute* phenotypes. For instance, loss of *RpS6*, a small subunit protein, causes a counterintuitive phenotype: extensive larval overgrowth (Lin *et al.* 2011). Studies to determine which tissues normally require RpS6 to restrict growth showed that prothoracic glands of *RpS6* mutants do not function properly. The consequent lower level of the hormone ecdysone, which promotes larval developmental progression and molts, extends the period of larval development and feeding. *RpS6* mutant larvae feed longer and grow abnormally large (Lin *et al.* 2011). It is unclear whether the prothoracic gland is particularly sensitive to the skewed stoichiometry of ribosomal proteins in *RpS6* mutants or whether RpS6 has a more specific function in this tissue, such as regulation of ecdysone synthesis directly. A specific role would be consistent with the recently proposed view that the ribosome is not a uniform constitutively active complex. Instead ribosomes are composed of variable subunits that facilitate unique translation regulation of mRNA subsets (Xue and Barna 2012). In support of this concept, mice mutant for a large subunit protein, *RpL38*, have specific homeotic transformations due to failed translation of, and 80S association with, a certain subset of Hox gene mRNAs (Kondrashov *et al.* 2011).

Here we report detailed genetic and biochemical studies of another protein that regulates ribosome assembly and has a distinctive phenotype beyond reduced growth at the cell-autonomous level. This study follows from our previous characterization of flies carrying an allele of *Drosophila Nucleostemin 3* ($ns3^{G0431}$) (Kaplan *et al.* 2008). These flies are developmentally delayed during larval stages, have partial recessive lethality, eclose late, and are small. Nucleostemin 3 (NS3) is closest in sequence to yeast Lsg1p, the protein necessary for recycling the 60S export protein Nmd3 to the nucleus (Kallstrom *et al.* 2003; Hedges *et al.* 2005). It therefore seemed reasonable that the *ns3* loss-of-function phenotypes are due to an overall reduction in protein synthesis like a typical *Minute*. However, we found that homozygous mutant clones of *ns3* were not small, indicating non-cell autonomous rescue of mutant cells by cells elsewhere that have functional NS3. Remarkably, expression of *ns3-YFP* in neurons using a *elav-gal4* driver was capable of nearly completely rescuing the phenotype (Kaplan *et al.* 2008). Here we show that two newly analyzed larval lethal alleles of *l(1)2Ad* are strong loss-of-function alleles of *ns3*. The lethality of these alleles, and *ns3-RNAi* studies, indicates additional cell-autonomous growth roles of NS3. The hypomorphic allele $ns3^{G0431}$ reveals critical growth-promoting roles of neurons. We conclude that *ns3* has both cell-autonomous and non-cell-autonomous growth-promoting roles.

Materials and Methods

Percentage protein similarity and phylogenetic analyses

Percentage protein similarity over the entire length of individual fly NS members *vs. S. cerevisiae* Lsg1p was determined using EMBOSS Stretcher. A phylogenetic tree of fly NS members and yeast and human Lsg1p proteins was generated by ClustalW2 (Larkin *et al.* 2007). The distance value of each branch shows the number of substitutions as a proportion of the length of the alignment (gaps excluded).

Yeast rescue experiments

NS3 DNA was amplified by PCR from UAST–NS3–YFP using oligos: 5-GCCACTAGTACCATGGGCAAAAAGAACAAGGG and 5′-TTTTAAGCTTCTAGTTAATTAAGTGCTCGTC CAGGTGCGAGA for cloning into pRS415–GPD or 5′-GGCA CTAGTAAAATGGGCAAAAAGAACAAGGGC and 5′- GCCAAGCT TCAGTGCTCGTCCAGGTGCG for cloning into pRS425–GPD. *NS1* DNA was PCR amplified from complete cDNA AT23067 using primers 5′-GGCACTAGTAAAATGGCTTTAAAAAGGTTGA AGACC and 5′-GCCAAGCTTATTCAATCACATAGTCC. *NS2* DNA was PCR amplified from complete cDNA SD10213 with primers 5′-GGCACTAGTAAAATGCCAAAGGTACGCAGCACC and 5′-GC CAAGCTTACGCGTCCTTCTTTTTGTTTCTATTGC. *NS4* DNA was PCR amplified from complete cDNA LD10773 with primers 5′-GGCACTAGTAAAATGCCACAGCAACGGCGC and 5′-GCCAAGCTTAATCGTCCTCCAGCAGAGC. The products were digested with *Spe*I and *Hin*dIII and cloned into pRS415–GPD or pRS425–GPD (Mumberg *et al.* 1995). The various *NS* clones, wild-type yeast *LSG1*, or empty vector was transformed into AJY1171 [*MATalpha lsg1*Δ::*KanMX his3Δ1 leu2Δ0 ura3Δ0 lys2Δ0* containing plasmid pAJ626 (*LSG1 URA3 CEN*)]. Transformants were selected on Leu^- medium and restreaked onto Leu^- medium containing 5-FOA and incubated for 5 days at 30°.

Drosophila culture and strains utilized

Drosophila were cultured on standard molasses media at 25° except where indicated. The following fly lines were acquired from the Bloomington *Drosophila* Stock Center: *ddc-gal4* (Li *et al.* 2000), *ple/th-gal4* (Friggi-Grelin *et al.* 2003), $l(1)2Ad^1$, $l(1)2Ad^3$, *Df(1)BSC719*, $ns3^{G0431}$, *P{GAL4-Act5C.FRT.P}*, *P{UAS-mCD8::GFP.L}LL4*, *P{hsFLP}22*; *Pin [1]/CyO*, *c061-gal4*, and *uas-lamin-gfp*. The *dtrh-gal4* was a gift from Dr. Ed Kravitz (Alekseyenko *et al.* 2010). The *isoD1* line was a gift from Drs. Daryl Gohl and Tom Clandinin (Gohl *et al.* 2011).

Generation of expression vectors and transgenic flies

For the K350N antimorphic version of *ns3*, a Gateway entry clone pDONR207 (Invitrogen) containing *ns3* was mutated with point mutations (K to N) using a QuikChange XL

site-directed mutagenesis kit (Stratagene). *LSG1* cDNA was amplified from vector pAJ2229 (Arlen Johnson) and cloned into entry clone pDONR207. *Ns3*(K350N) and *LSG1* were then cloned into pTVW and pTW, respectively, using site-specific recombination according to the manufacturer's Gateway cloning protocol. The resulting expression vectors were injected into *yw* embryos to generate transgenic fly lines.

Fly weight, developmental time to eclosion, and percentage viability studies

The Gal4 drivers (*dtrh-gal4*, *ddc-gal4*, *th-gal4*) were all back-crossed five times with the isogenic line isoD1 to reduce background genetic effects (Gohl *et al.* 2011), and a recombinant *dtrh*-gal4, *th-gal4* line was subsequently created. Males of this strain were crossed to virgin females of the genotype $ns3^{G0431}$*/FM7i*, *Act* > *GFP*; *uas-ns3-YFP* for 6–8 hr in collection bottles, where embryos were laid on standard molasses/agar plates. The embryos were aged for 24 hr at 29° until hatching, then 40 non-GFP (*ns3/Y* and *ns3/*+) larvae were transferred to vials containing standard molasses medium, in triplicate. Vials were placed at 29° and the number of flies eclosing daily was scored. Fly weight measurements were carried out as previously described (Kaplan *et al.* 2008). Survival to adulthood of $ns3^{G0431}$/Y males with and without expression of *ns3-yfp* in DA, serotonergic (5-HT), and DA plus 5-HT neurons was quantified by dividing the total $ns3^{G0431}$/Y male flies that eclosed over the number expected to eclose (40, the number of $ns3^{G0431}$/+ females eclosed) from three replicates of vials that carried 40 $ns3^{G0431}$/Y and $ns3^{G0431}$/+ larvae.

Ns3 allele molecular mapping

$ns3^{l(1)2Ad1}$ is an allele containing a deletion of 8 bp in the second exon (the deleted nucleotides are flanked by dashes: TACG-TAAAGGAG-GTGG). This is predicted to result in a truncation after 198 of the 606 amino acids (33%), followed by three missense amino acids and an early stop. The truncated protein would not contain the putative GTP-binding domain (as predicted by InterPro Scan), which includes amino acids 349–396. The $ns3^{l(1)2Ad3}$ allele has a deletion of 46 bp in the second exon (the deleted nucleotides are flanked by dashes: GCCG-AGGAGCTAGTGCGAG CCGAGAACGAGGCATTTCTCGACTGGCGCCG-CGACCTGGCG). This may result in a truncation after 126 of the 606 amino acids (21%), followed by 12 missense amino acids and an early stop. This predicted truncated protein would not contain the putative GTP-binding domain. $ns3^{G0431}$ is an insertion of P{lacW} into the 5′-UTR (insertion exists in the following sequence at the site of the slash: TGATTGT CAAAAACACGTGCAATGTTTGCCC/G).

Creation of recombinant NS3–maltose-binding protein and GTPase assay

Full-length *ns3* was cloned into a pMal–p5X vector that contains a maltose-binding protein (MBP) tag. MBP-tagged NS3 protein (NS3–MBP) was expressed in BL21 codon+DE competent cells and purified under the following conditions. The culture was grown at 37° in LB amp supplemented with glucose until an $OD_{600\ nm}$ of 0.5 was reached. The flask was then cooled to 16° and induced with 0.1 mM IPTG overnight. The cells were pelleted and resuspended in 25 ml column buffer [20 mM Hepes, 200 mM NaCl, 1 mM EDTA, protease inhibitors (Sigma P8465), and 1 mM DTT]. Cell lysis was achieved by the addition of lysozyme (0.2 mg/ml) for 30-min on ice. The lysate was then sonicated, Triton X-100 was added to a final concentration of 1%, and the lysate was centrifuged for 30 min at 48,384 × *g* at 4°. The supernatant was then applied to a column containing 1 ml of Amylose Resin (New England BioLabs) and gently rotated overnight at 4°. The supernatant was then allowed to flow through the column (Kontes flex column 1 × 10 cm) by gravity, the amylose NS3–MBP carrying resin bed was washed with column buffer four times, and NS3–MBP was eluted with multiple 500-μl aliquots of column buffer containing 10 mM maltose. The various elutions were tested for the presence of NS3–MBP via SDS–PAGE analysis, and the elutions containing NS3–MBP were pooled. Two major bands were seen, 112 (NS3–MBP) and 42 kDa (MBP). Two fractionation steps were then applied. First, an Amicon Ultra100 was used to separate NS3–MBP (112 kDa) from MBP (42 kDa). Second, the <100-kDa flow-through from the Amicon Ultra100 fraction was further purified with an Amicon Ultra30. The ≥100-kDa, 112-kDa NS3–MBP containing retentate, from fractionation 1 and the ≥30-kDa, 42-kDa MBP containing retentate from frationation 2 were used for the GTPase assay. NS3–MBP and MBP concentrations were measured by Bradford protein assay. The GTPase activities of NS3–MBP and MBP were determined using Innova Biosciences GTPase Kit following the manufacturer's protocol. A standard curve was made using P_i standards and was used for calculation of amount of released P_i and GTPase activity.

NS3 antibody creation, purification, and Western analysis

Two rabbits were immunized against the C terminus of NS3 (amino acids 306–606) (Josman Labs). Raw serum from the rabbit recognizing the 70-kDa NS3 via Western analysis was then purified with a NS3–MBP bound column (AminoLink Plus Immobilization Kit, Pierce) and subsequently used for the immunolocalization (1:250) and Western analyses herein (1:250). For Western analyses, standard procedures were applied using embryonic protein extracts obtained via microcentrifuge tube–pestle homogenization in PIPES buffer [80 mM PIPES, pH 7.0, 5 mM EGTA, 5 mM $MgCl_2$, and a tablet of protease inhibitors (Roche, EDTA free) at 1× strength] on ice. Samples were then centrifuged at maximum speed at 4° and supernatant was transferred to a new tube and kept on ice or stored at −80° until preparation for SDS–PAGE.

Table 1 YRG family members in yeast, fly and human with documented or likely roles in ribosomal biogenesis

YRG member	Implication in growth and/or role in ribosome assembly
Nug1 (*S.c.*)	Nuclear export of 60S ribosomal subunits (Bassler *et al.* 2001; Bassler *et al.* 2006)
NS1 (*D.m.*)	Nucleolar export of large ribosomal subunits (Rosby *et al.* 2009)
GNL3L (*H.s.*)	Nucleolar pre-rRNA processing (Du *et al.* 2006; Rosby *et al.* 2009; Yasumoto *et al.* 2007; Zhu *et al.* 2009)
GNL3/NS (*H.s.*)	60S pre-rRNA processing (Cladiere *et al.* 2006; Tsai and McKay 2002)
Nog2/Ngp1 (*S.c.*)	60S export from nucleolus to nucleoplasm (Saveanu *et al.* 2001)
NS2 (*D.m.*)	Decreased function alters ratio of rRNA in nuclear *vs.* cytoplasm (Matsuo *et al.* 2011)
GNL2/Ngp1 (*H.s.*)	nucleolar localization (Shin *et al.* 2004)
Lsg1 (*S.c.*)	60S nuclear export to cytoplasm (Hedges *et al.* 2005; Kallstrom *et al.* 2003)
NS3 (*D.m.*)	Growth, rescues yeast *lsg1* null mutant (Kaplan *et al.* 2008)
hLsg1 (*H.s.*)	Cell growth and viability (Reynaud *et al.* 2005)
NS4 (*D.m.*)	No phenotype found for putative allele (Kaplan *et al.* 2008)
GNL1 (*H.s.*)	Shuttles between nucleolus to nucleoplasm; controls growth (Boddapati *et al.* 2012)
Mtg1 (*S.c.*)	Mitochondrial translation (Barrientos *et al.* 2003)
CG17141 (*D.m.*)	No known roles
Mtg1 (*H.s.*)	Rescues yeast *mtg1* null mutant (Barrientos *et al.* 2003)

The YRG family members expanded in eukarya from a single ancestor resembling modern prokaryotic YlqF. All family members carry a circularly permuted GTPase domain and most, if not all, have specific roles in ribosomal biogenesis.

Microscopy and image analysis

Larval CNS, salivary glands, and imaginal discs were prepared for imaging as previously described with PBS containing 0.1% Triton X-100 (PBT), overnight incubations in primary antibody, and 4-hr incubations in secondary antibody at room temperature (Wu and Luo 2006). F-actin staining in Supporting Information, Figure S2 was carried out by incubating tissues in AlexaFluor 594 conjugated Phalloidin (Invitrogen) at a 1:40 concentration for 20 min in the first PBT wash following secondary antibody incubation. The following primary antibodies were employed for these studies: anti-RpL13 (Abcam), anti-RpS6 (Cell Signaling), and anti-Tyrosine Hydroxylase (ImmunoStar). All images were made on a confocal Leica TCS SP2 laser-scanning microscope. The average pixel intensity of RpL13, RpS6, and NS3 (Figure 5 and Figure S2) was obtained using image J (Schneider *et al.* 2012). To quantify cytoplasmic RpL13 and RpS6 levels, ellipses were manually drawn proximal, but external to, nuclei as defined by DAPI or lamin–GFP. Ellipses were then converted to curved lines with the "convert region to line" plugin and average pixel intensities for ribosomal proteins under the curved line were measured. The stochastic expression of the *c061-gal4* driver in the salivary gland made it possible to compare the outcome of *ns3* knockdown to neighboring "wild-type" cells that did not produce Gal4. Each *c061-gal4* salivary gland typically had 2–10 cells that did not express Gal4. Gal4*/ns3-dsRNA*-expressing cells were identified by the presence of lamin–GFP. The average pixel intensity of RpL13 and RpS6 in wild-type cells not expressing *ns3-dsRNA* (non-lamin–GFP) was normalized by the average pixel intensity of ribosomal protein staining in neighboring *ns3-dsRNA* (lamin–GFP-positive) cells. Equivalent measurements were carried out in control salivary glands where *c061-gal4* drove expression of only *uas-lamin-gfp*. Quantification of the level of NS3 in DA neurons of wild-type *vs.* $ns3^{G0431}$ (Figure S3) was carried out by manually drawing four lines in the cytoplasm of cells carrying the DA marker tyrosine hydroxylase (TH) and then measuring the average pixel intensity of NS3 staining. This value was normalized by dividing it by the average pixel intensity of NS3 in surrounding, TH−, cells. These control values were obtained by manually drawing four boxes in surrounding brain tissue and measuring average pixel intensity.

Results

NS3 is the functional ortholog of yeast Lsg1

In eukaryotic evolution, a clade of GTPases expanded from an ancient prokaryotic protein that resembled modern YlqF, an essential GTPase that promotes ribosome assembly (Leipe *et al.* 2002; Reynaud *et al.* 2005; Uicker *et al.* 2006). Most members of the YlqF-related GTPase (YRG) family have clear roles in ribosome biogenesis, particularly in the maturation and movement of ribosome subunits from nucleoli to the cytoplasm (Table 1) (Reynaud *et al.* 2005). The expansion of several ribosome biogenesis factors during eukaryotic evolution has evidently facilitated the compartmentalization of ribosome biogenesis steps in the modern eukaryotic cell (Reynaud *et al.* 2005).

The *S. cerevisiae* YRG member Lsg1p is a cytoplasmic GTPase that is associated with nascent 60S subunits (Figure 1A). An apparent gene duplication of *LSG1* in coelomate evolution created one paralog that has the highest similarity to *LSG1* and another that diverged in sequence (Reynaud *et al.* 2005). Based on protein sequence similarity, the likely ortholog of Lsg1p in *Drosophila* is nucleostemin 3 (53.1% similar), with nucleostemin 4 (40.6% similar) being a divergent paralog (Table 1 and Figure 1A).

To further validate that NS3 is the functional ortholog of Lsg1p, we transformed *LSG1*, *Drosophila nucleostemins 1-4*, or empty vector into the *lsg1*Δ yeast mutant containing a *LSG1 URA3* vector. The *LSG1 URA3* vector was eliminated on 5-FOA-containing medium, which is toxic to cells containing a *URA3* gene. Strains transformed with *ns3* partially

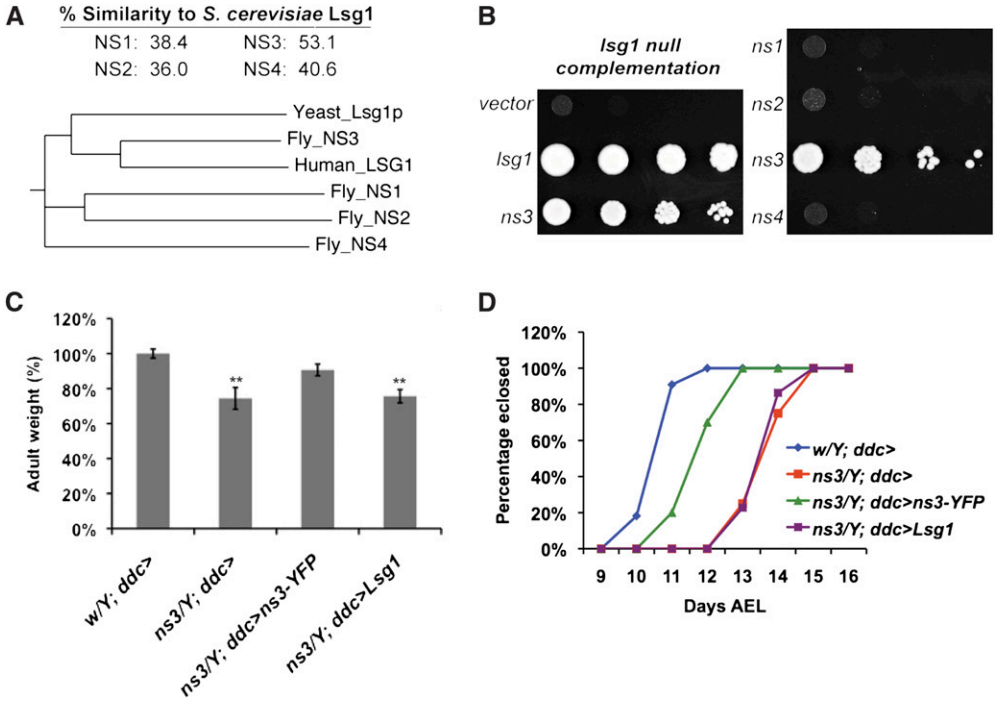

Figure 1 *Drosophila* NS3 partially rescues yeast *lsg1*Δ lethality. (A) Percentage similarity and phylogenetic tree of the *Drosophila* NS family. Of the four *Drosophila* NS family members, NS3 has the strongest protein sequence similarity to yeast Lsg1p (EMBOSS stretcher). A multiple alignment and phylogram tree of the *Drosophila* NS family, yeast Lsg1p, and human Lsg1 were generated by ClustalW2 (Larkin *et al.* 2007). The distance value of each branch shows the number of substitutions as a proportion of the length of the alignment (gaps excluded). Sequence homology of NS3 with yeast and human Lsg1 leads to their clustering within the phylogeny. (B) Yeast *lsg1*Δ cells were complemented by transformation of *LSG1* and *Drosophila ns3*, but not by transformation with *Drosophila ns1*, *ns2*, or *ns4*. (C) *LSG1* driven by the *ddc-gal4* driver did not rescue the decreased body weight of the $ns3^{G0431}$ mutant. The average adult male weight, derived from three groups of 10 flies, is expressed as a percentage of the average weight of negative control flies that carried only *ddc-gal4*. Expression of *uas-ns3-yfp* with *ddc-gal4* rescued the $ns3^{G0431}$ mutant phenotype to the size of wild-type flies, but expression of *uas-LSG1* did not. (D) *LSG1* driven by the *ddc-gal4* driver did not rescue the delayed development of the $ns3^{G0431}$ mutant. The number of eclosed flies was scored daily. The number of $ns3^{G0431}$ males eclosed per day is plotted as the percentage of the total $ns3^{G0431}$ males eclosed. Expression of *uas-ns3-yfp* with *ddc-gal4* partially rescued the developmental delay of the $ns3^{G0431}$ mutant so that eclosion occurred closer to the time of negative-control wild-type flies that carried only *ddc-gal4*. Expression of *uas-LSG1* using *ddc-gal4* did not rescue $ns3^{G0431}$ developmental delay; these flies were as developmentally delayed as $ns3^{G0431}$/Y; *ddc-gal4* flies.

rescued *lsg1*Δ lethality. In contrast, *ns1*, *ns2*, and *ns4* did not rescue lethality of *lsg1*Δ (Figure 1B). This suggests that NS3 is a functional ortholog of Lsg1p.

Yeast *LSG1* expression was unable to rescue mutant *ns3* flies. We previously demonstrated that fly *ns3* mutants ($ns3^{G0431}$) could be rescued by the expression of wild-type *ns3-yfp* using the *ddc-gal4* driver (Kaplan *et al.* 2008). Expression of *LSG1* with this same driver was not capable of rescuing the *ns3* decreased fly size (Figure 1C) or the *ns3* developmental delay (Figure 1D). We suggest that NS3 acquired unique features during metazoan evolution that preclude Lsg1p from rescuing an NS3 deficiency. This might have entailed alterations that enable unique protein localization properties, as discussed below.

Alleles of l(1)2Ad are strong loss-of-function alleles of ns3 and are larval lethal

The $ns3^{G0431}$ mutation causes phenotypes common to the *Minute* phenotypic class: developmental delay, small cell size, and small adults (Lambertsson 1998; Marygold *et al.* 2007). The $ns3^{G0431}$ fly is not a typical *Minute* as its growth defects are non-cell autonomous and caused by defective neuronal signaling (Kaplan *et al.* 2008). However, a purely non-cell-autonomous growth-control function of NS3 is unlikely based on the following. First, yeast and human orthologs of NS3 have strong effects on cell growth and viability (Hedges *et al.* 2005; Reynaud *et al.* 2005). Second, expression of a shRNA targeting *ns3* either ubiquitously (*tubulin-gal4*; 100% lethal) or in neurons (*elav-gal4*; 100% lethal) causes lethality exceeding that of the $ns3^{G0431}$ mutant, which has "escapers" that make it to adulthood.

To clarify the roles of *ns3*, we sought stronger mutant alleles. FlyBase lists several genetic loci that were mapped genetically or cytologically, but not yet to a nucleotide coordinate. *Ns3* falls within cytological band 2A4. In a search of genetic aberrations listed on FlyBase that are near or within cytological band 2A4, we acquired 19 candidate lines from the Bloomington Stock Center with lesions possibly falling within the *ns3* locus.

We performed complementation tests with the various candidate alleles. $ns3^{G0431}$/Y males were crossed to candidate females carrying an X chromosome mutation, often balanced over FM7. Since homozygous female $ns3^{G0431}$ mutants are lethal and developmentally delayed, we first looked for complementation by virtue of the presence of $ns3^{G0431}$/X females among early eclosing flies. We then looked for a failure to complement, deduced from the absence of $ns3^{G0431}$/X females until several days after their siblings had eclosed. These studies revealed that $l(1)2Ad^{1}$ and $l(1)2Ad^{3}$ are alleles of *ns3*. Sequencing the three alleles of *ns3* identified the $ns3^{l(1)2Ad1}$ lesion as an 8-bp deletion in the second exon. This causes a frameshift and the

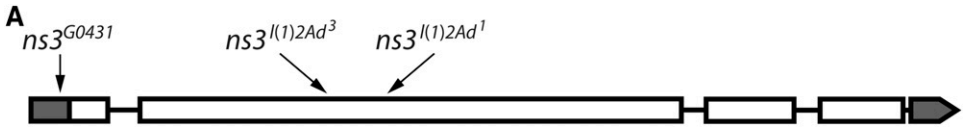

B

PARENT CROSS	FM7i/Y	ns3/FM7i	ns3/Y	male viability	ns3/ns3	female viability
$ns3^{G0431}$/Y X $ns3^{G0431}$/FM7i	65	112	88	78%	0	0%
$ns3^{G0431}$/Y X $ns3^{l(1)2Ad1}$/FM7i	53	58	0	0%	13	22.4%
$ns3^{G0431}$/Y X $ns3^{l(1)2Ad3}$/FM7i	26	74	0	0%	12	16.2%
$ns3^{G0431}$/Y X Df(1)BSC719	86	115	0	0%	0	0%

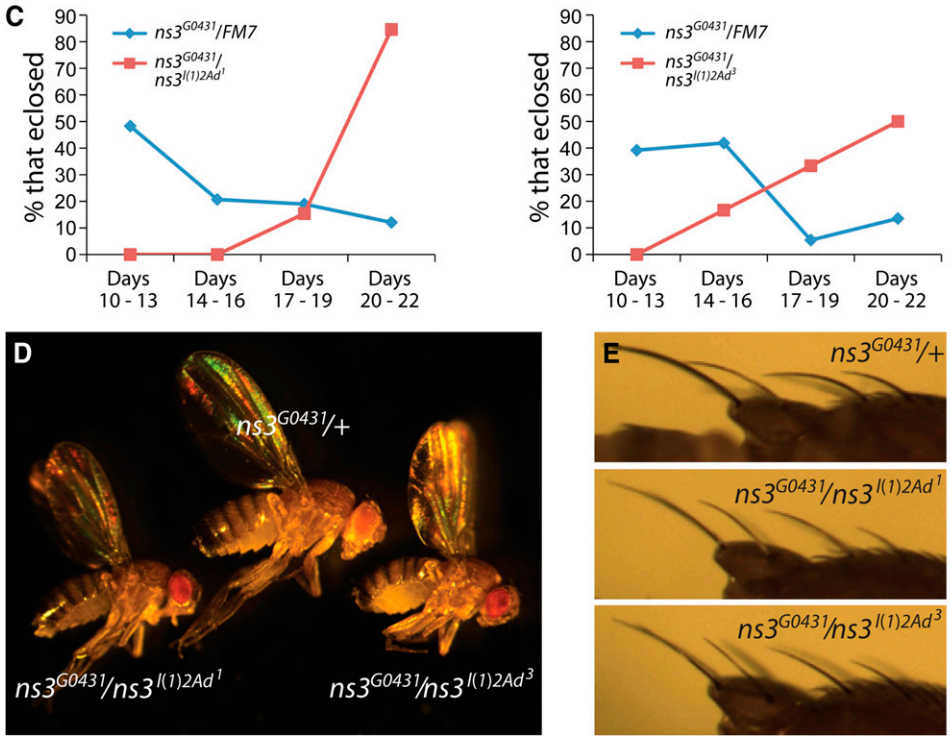

Figure 2 *l(1)2Ad* alleles map to the *ns3* locus and mimic developmental delay and *Minute*-like phenotypes. (A) Map indicating positions of *ns3* aberrations leading to loss-of-function. Alleles $l(1)2Ad^1$ and $l(1)2Ad^3$ are small deletions mapping to the second exon and the *G0431* allele is a *P*-element insertion into the 5′-UTR. (B) All three *ns3* alleles are necessary for viability. $ns3^{G0431}$/Y males were crossed to heterozygous $ns3^{l(1)2Ad1}$/FM7i, $ns3^{l(1)2Ad3}$/FM7i, and $ns3^{Df(1)BSC719}$/FM7i females. Male and female percentage viability is the number of mutant animals divided by the number of sibling $ns3^{G0431}$/FM7i that emerged. (C) The surviving $ns3^{l(1)2Ad3}$/$ns3^{G0431}$ (N = 12) and $ns3^{l(1)2Ad1}$/$ns3^{G0431}$ (N = 13) females eclose later than sibling $ns3^{G0431}$/FM7i females (N = 58 and 74, respectively) and are thus developmentally delayed. (D) $ns3^{l(1)2Ad3}$/$ns3^{G0431}$ and $ns3^{l(1)2Ad1}$/$ns3^{G0431}$ females are small in size. (E) $ns3^{l(1)2Ad3}$/$ns3^{G0431}$ and $ns3^{l(1)2Ad1}$/$ns3^{G0431}$ females have slender bristles mimicking the *Minute* phenotype.

introduction of an early stop codon, possibly creating a protein abnormally shortened by 33%. The $ns3^{l(1)2Ad3}$ lesion is a 46-bp deletion in the second exon, also causing a frameshift. This allele is expected to make a truncated protein only 22% the length of wild type. Neither $ns3^{l(1)2Ad1}$ nor $ns3^{l(1)2Ad3}$ alleles are expected to code for a protein with a functional GTPase. The $ns3^{G0431}$ allele is a *P-element* insertion in the 5′-UTR (Figure 2A).

The alleles $l(1)2Ad^1$ and $l(1)2Ad^3$ were previously characterized as first-instar lethal. In mosaic analyses with these alleles the gene was necessary for female germline viability (Perrimon *et al.* 1989). Our confirmation that 0% of $ns3^{l(1)2Ad1}$/Y and $ns3^{l(1)2Ad3}$/Y males survive to adulthood (Figure 2B) shows that they have less function than $ns3^{G0431}$, which allows 78% of adult males to survive. In our previous studies we observed some $ns3^{G0431}$ homozygous females, but we no longer see them. Perhaps the $ns3^{G0431}$-bearing chromosome has acquired another aberration that affects female viability. If this is the case it would likely be near the $ns3^{G0431}$ insertion, since $ns3^{G0431}$ is lethal over the deficiency *Df(1)BSC719* (Figure 2B)—the female-specific lethality must be closely linked. We do find $ns3^{l(1)2Ad1}$/$ns3^{G0431}$ and $ns3^{l(1)2Ad3}$/$ns3^{G0431}$ *trans*-heterozygotes. These flies are developmentally delayed (Figure 2C) and are small (Figure 2D). Given that our current $ns3^{G0431}$ stock yields few to no homozygous females (Figure 2B), we performed subsequent analyses with hemizygous males.

In our previous studies, flies carrying $ns3^{G0431}$ males were developmentally delayed and small due to nonautonomous growth-controlling roles of *ns3* (Kaplan *et al.* 2008). We suspect that this less-lethal phenotype is due to the allele retaining partial function. In contrast, the strong alleles $ns3^{l(1)2Ad1}$ and $ns3^{l(1)2Ad3}$ illustrate the expected requirement for NS3 in all cells. These two mutations prevent female germline viability (Perrimon *et al.* 1989) and are 100% lethal. Given the likely function of NS3 in ribosome

biogenesis, strong alleles of *ns3* should be considered a class of *Minutes*. Consistent with this designation, bristles of $ns3^{l(1)2Ad3}/ns3^{G0431}$ and $ns3^{l(1)2Ad1}/ns3^{G0431}$ are slender and short in length, a classic *Minute* phenotype thought to result from suboptimal protein synthesis (Figure 2E).

NS3 is a functioning GTPase and inactivation of this domain confers antimorphic activity

Unlike conventional GTPases that contain five G-domain motifs ordered G1–G2–G3–G4–G5, the YRG family of GTPases (including Lsg1p) carry "circularly permuted" G-motifs in the order G4–G5–G1–G2–G3 (Figure 3A). Mutations within the putative GTP-binding domain of yeast Lsg1 cause a strong antimorphic effect, preventing ribosomal subunit export from the nucleus and stalling growth (Kallstrom *et al.* 2003; Hedges *et al.* 2005). This suggests that the GTPase domain is catalytically active and relevant for function, despite the atypical ordering of G-motifs. To directly test the activity of the permuted GTP-binding motifs in NS3, we purified recombinant NS3–MBP (maltose-binding protein) from *E. coli* and performed *in vitro* GTPase assays. A linear relationship was observed between the concentration of NS3–MBP and the amount of GTP hydrolyzed within 1 hr at 37° (Figure 3B), while the negative-control MBP protein was incapable of GTP hydrolysis. NS3's intrinsic GTP hydrolysis rate, K_{cat} 4.27 ± 0.59 min^{-1}, is on par with that of heterotrimeric G-proteins (K_{cat} 3–5 min^{-1}) (Kaziro *et al.* 1991), although relatively high compared to some circularly permuted GTPases (K_{cat} ~0.2 min^{-1}) (Daigle and Brown 2004; Himeno *et al.* 2004; Bassler *et al.* 2006; Cladiere *et al.* 2006) and canonical Ras and Rab GTPase members (K_{cat} <0.01 min^{-1}) (Kaziro *et al.* 1991). It is unknown whether GTPase activities of Lsg1/NS3 orthologs can be stimulated by GTPase-activating proteins (GAPs) or other factors that can increase catalytic rate >100-fold (Kaziro *et al.* 1991; Bernards and Settleman 2004). For instance, the K_{cat} of *E. coli* YRG member YjeQ is increased ~500-fold in the presence of small ribosomal subunits (Daigle and Brown 2004).

To further study the GTPase function of NS3, we introduced into flies a UAS-controlled *ns3* transgene carrying point mutations in the GTPase domains. The "K350N" NS3 mutation we employed falls within the conserved G1 motif (GX4GKS/T) of the GTPase domain (Figure 3A). Previous studies of other GTPases have shown that mutating this lysine residue reduces the GTPase catalytic activity. For example, mutating the lysine to alanine (K220A) in YjeQ, an *E. coli* circularly permuted GTPase, reduced its K_{cat} by ~2.5-fold (Daigle *et al.* 2002). Hydrogen bonding provided by the K16 residue in H-Ras is thought to coordinate the γ-phosphate of GTP for nucleophilic attack by a water molecule (Pai *et al.* 1990). A H-Ras K16N mutant, which corresponds to the mutation we created in NS3 (K350N), caused a ~100-fold reduction in affinity for GDP and GTP, and its expression in yeast suppressed cell growth (Sigal *et al.* 1986). Thus, these previous studies suggest that replacing the NS3 lysine at position 350 with asparagine will create a mutant protein defective in the binding, coordination, and catalysis of GTP. The corresponding K350N mutation in *S. cerevisiae* Lsg1 is lethal and antimorphic (Hedges *et al.* 2005).

When a wild-type *ns3-YFP* transgene was expressed in $ns3^{G0431}$ flies, using the *ddc-gal4* driver, the delayed development and small body size phenotypes were rescued (Kaplan *et al.* 2008). To test whether our new *ns3-K350N-yfp* behaved as an antimorph, we expressed it using the *ddc-gal4* driver. The effects of *ns3-K350N-yfp* were compared to flies expressing the wild-type *ns3-yfp* or to control flies that had no transgene. Consistent with antimorphic properties, expression of *ns3-K350N-yfp* using *ddc-gal4* phenocopied the $ns3^{G0431}$ mutant phenotype, causing significantly increased developmental time to eclosion and decreased adult body size (Figures 3, C and D). The co-expression of wild-type *ns3-yfp* from a single transgene with *ns3-K350N-yfp* rescued the fly size and developmental timing defects of *ns3-K350N-yfp* alone, thus validating that the K350N protein variant behaved as an antimorph (Figures 3, C and D). Expression of *ns3-yfp* from two different transgenes provided an even stronger rescue of the *ns3-K350N-yfp* phenotypes, although quantitation would be necessary to determine whether more NS3–Yfp is produced when expressed from two *vs.* a single transgene. *Ns3-K350N-yfp* expression via *ddc-gal4* was unable to rescue the $ns3^{G0431}$ delayed developmental time to eclosion and decreased adult body size phenotypes (Figures 3, E and F), validating that it does not have full wild type functionality.

NS3 is necessary for cell-autonomous growth control and localizes to cytoplasmic puncta and nuclear and cellular peripheries

We next sought to characterize the tissue expression pattern and subcellular localization of NS3. Using newly made antibodies against the fly protein, we visualized NS3 in the imaginal wing disc and salivary gland (Figures 4, A–K). In parallel with these NS3 localization studies, we expressed a UAS-driven shRNA directed against *ns3* in discrete subsets of cells within a tissue. This was performed using a heat-shock-driven FLP recombinase and an *actin-gal4* that cannot produce Gal4 unless FLP removes a FRT-flanked transcriptional stop upstream of the *gal4* ORF. The stochastic nature of the transcriptional stop removal leads to a mosaic expression pattern of *gal4*, which subsequently drives expression of cell surface GFP (*uas-mCD8-GFP*) and *ns3-shRNA* simultaneously in the same subset of cells. In response to *ns3-shRNA*, the amount of NS3 protein is clearly reduced in the GFP-marked *ns3-shRNA* expressing cells in the wing disc (Figures 4, A–D) and salivary gland (Figures 4, E–J). Note that in the salivary gland, decreased *ns3* reduces cell size (Figures 4, E–J), presumably because decreased protein production interferes with growth. The largest cross-section of wild-type salivary gland cells had an area of 4096.7 ± 176.0 μm^2. In contrast, cells expressing *ns3-RNAi*, measured in an

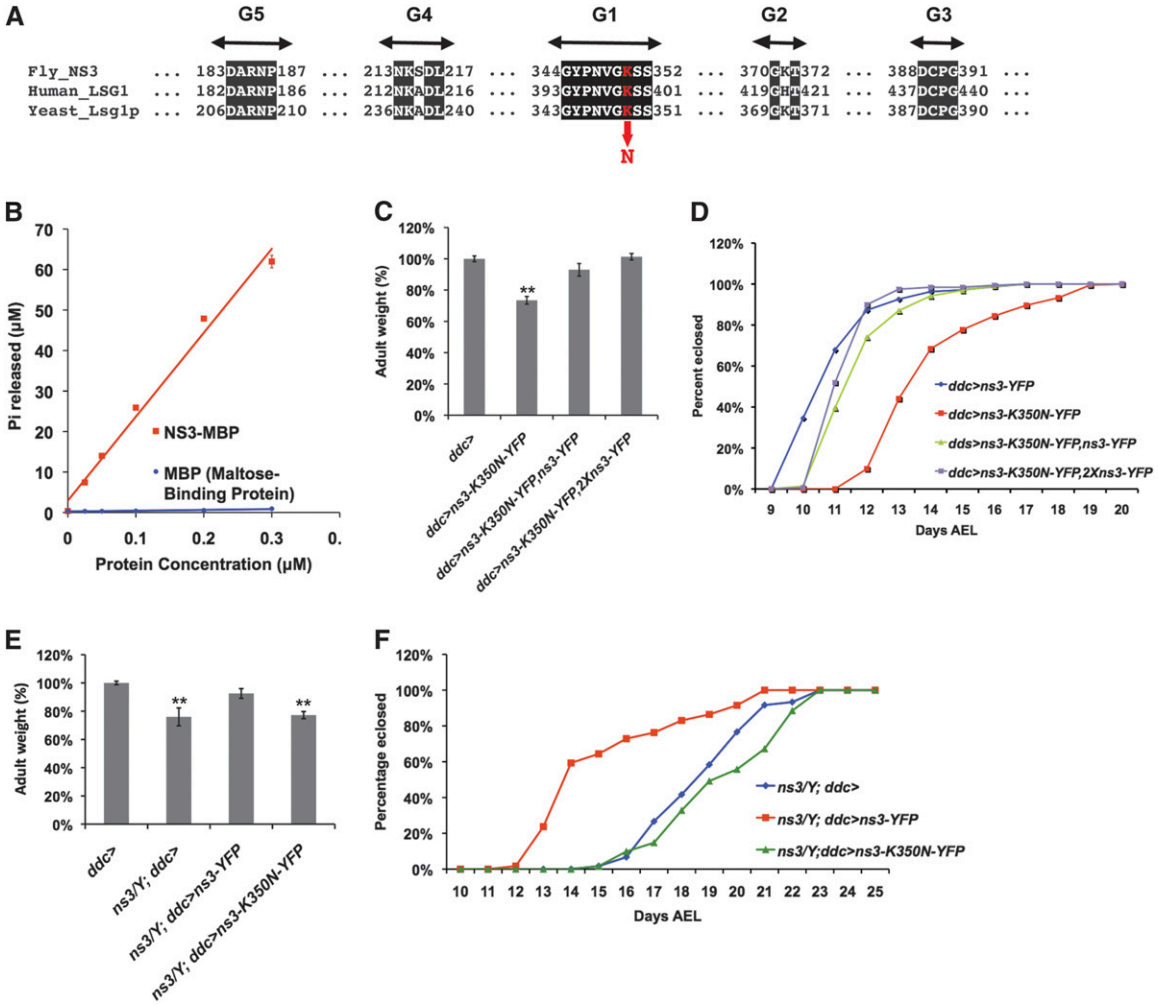

Figure 3 NS3 exhibits GTPase activity and mutating an invariant lysine residue in the GTPase domain confers antimorphic activity. (A) Conserved circularly permuted GTP binding domains among NS3 homologs in human and yeast. The location of the antimorph creating residue (*ns3-K350N-yfp*) is indicated in red. (B) NS3 exhibits GTPase activity *in vitro*. (C) Expression of antimorphic *ns3-K350N-yfp* with *ddc-gal4* caused decreased body weight ($P < 0.05$), which can be rescued by expression of wild-type *ns3-yfp*. The average adult male weight, derived from three groups of 10 flies, is expressed as a percentage of the average weight of negative-control flies that carried only *ddc-gal4*. (D) Expression of antimorphic *ns3-K350N-yfp* via *ddc-gal4* caused developmental delay (red line), which can be rescued by expressing wild-type *ns3-yfp* (green and purple lines). The number of eclosed flies was scored daily. The number of males eclosed per day is plotted as the percentage of the total males eclosed. (E) Decreased body weight of $ns3^{G0431}$ mutant can be rescued by expressing wild-type *ns3-yfp* ($P < 0.05$), but not the antimorphic *ns3-K350N-yfp* via *ddc-gal4*. The average $ns3^{G0431}$ adult male weight, derived from three groups of 10 flies, is expressed as a percentage of the average weight of negative-control flies that carried only *ddc-gal4*. (F) The $ns3^{G0431}$ developmental delay phenotype (blue line) can be rescued by expressing wild-type *ns3-yfp* (red line), but not the antimorphic *ns3-K350N-yfp* (green line), via *ddc-gal4*. The number of flies eclosed was scored daily. The number of males eclosed per day is plotted as the percentage of the total males eclosed.

identical manner, had a much smaller area of 1741.8 ± 367.7 μm^2. This difference is significant (*P*-value = 3×10^{-5}, student's *t*-test, $n = 13$ and 10 cells).

In wild-type cells, NS3 is present in the cytoplasm of diploid imaginal wing disc cells (Figure 4C) and polyploid salivary gland cells (Figure 4G). In the salivary gland, NS3 is not observed in the nucleus but is enriched proximal to, or coincident with, the nuclear envelope and plasma membrane (Figure 4J). NS3 is also present in cytoplasmic punctate structures (Figure 4, J, L, and M). Nuclear envelope proximal localization of NS3 was also observed on the oocyte nucleus of adult egg chambers and larval midgut cells, and cytoplasmic localization was observed in nurse and midgut cells (Figure S1). These patterns using our newly raised antibody represent NS3 localization as Western analysis indicates our antibody most strongly recognizes a protein of NS3's predicted molecular weight (70 kDa), and NS3–YFP expressed in the salivary gland (*c061 > ns3-yfp*) has identical localization patterns (cytoplasmic puncta and nucleus/cell membrane proximal) (Figure S1G and Figure S2). Membrane localization of NS3 and NS3–YFP may be unique to salivary gland cells, as it was not observed elsewhere. Yeast Lsg1 has been observed in the cytoplasm, although not in punctate structures or at the cell periphery (Kallstrom

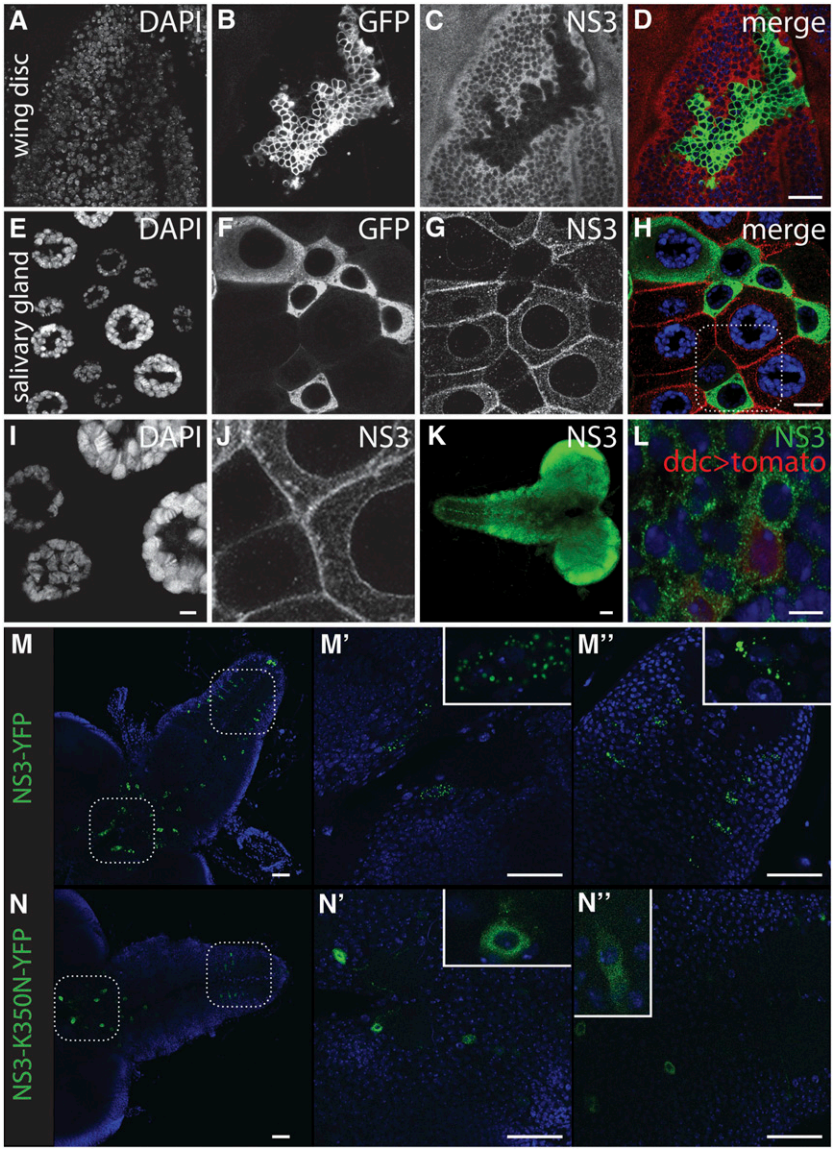

Figure 4 NS3 is localized to novel cytoplasmic punta, and the localization is dependent upon NS3 GTPase activity. (A–D) Image of an imaginal wing disc where an *actin-gal4*-expressing clone was induced to express *mCD8-GFP* and *ns3-dsRNA* and subsequently stained with an anti-NS3 antibody (A) DAPI, (B) mCD8-GFP, (C) anti-NS3, and (D) merged. Note the cytoplasmic NS3 that is substantially reduced in *ns3-dsRNA*-expressing, mCD8-GFP positive cells, confirming the specificity of the NS3 antibody. Scale bar, 20 μm. (E–H) A salivary gland expressing *mCD8-GFP* and *ns3-dsRNA* in a mosaic pattern. (E) DAPI, (F) mCD8-GFP, (G) anti-NS3, and (H) merged. Scale bar, 50 μm. (I–J) Higher magnification image of the salivary gland (see box in H) to show NS3 localization proximal or coincident with the nuclear envelope, cellular membrane, and within cytoplasmic puncta (I), DAPI (J), anti-NS3. Scale bar, 5 μm. (K) Larval CNS stained with anti-NS3 showing the ubiquitous distribution of the protein. Scale bar, 50 μm. (L) NS3 antibody staining in *ddc-gal4*; *uas-TdTomato*-labeled *ddc* neurons. NS3, green; *ddc* neurons, red; DAPI, blue. Scale bar, 5 μm. (M–M′′) Wild-type *ns3-yfp* driven by *ddc-gal4* demonstrating the punctate localization of NS3 in the cytoplasm. (N–N′′) *Ns3-K350N-yfp* expressed using *ddc-gal4* driver shows a diffuse pattern that extends into neurites. Scale bars, 50 μm.

et al. 2003; Hedges *et al.* 2005). Human hLsg1, like NS3, appears to exist in cytoplasmic foci and at the nuclear periphery. However, unlike NS3 localization, hLsg1 was observed in the nucleus colocalized with Cajal bodies as well as coincident with ER (Reynaud *et al.* 2005).

Our rescue of the *ns3*^{G0431} mutant with *ns3-yfp* expressed in neurons (*elav* > *ns3-yfp*) suggests hypersensitivity of neurons to low NS3 dose (Kaplan *et al.* 2008). *Ns3*^{G0431} could be rescued by expressing *ns3-yfp* using *ddc-gal4*, a driver that is active in most dopaminergic (DA) and 5-HT neurons (Li *et al.* 2000). Given that the majority of cells that express both *elav* and *ddc-gal4* drivers are DA and 5-HT neurons, NS3 may have a unique role in those cells. To investigate more closely whether NS3 has a special localization pattern in 5-HT and/or DA neurons, we compared staining levels of NS3 in *ddc-gal4*-expressing cells to neighboring cells that do not express *ddc-gal4* (Figure 4, K and L). To visualize *ddc-gal4*-expressing neurons, we drove *mtd-Tomato* with *ddc-gal4* and stained the larval CNS with our anti-NS3 antibody. NS3 appears ubiquitous throughout the larval CNS (Figure 4K), with no sign of unique NS3 patterns in *ddc*-expressing cells (Figure 4L). Thus, the special requirement for NS3 in *ddc* cells is not reflected in a visibly distinct protein localization pattern.

The GTPase domain is required for NS3 function (Figure 3). We observe an intriguing difference between NS3–YFP and NS3–K350N–YFP protein localization in neurons. NS3–YFP is strongly enriched in punctate structures, while NS3–K350N–YFP is much more diffuse and often spreads from the cell body into axons and dendrites (Figure 4, M and N). GTP coordination or hydrolysis may be necessary for proper NS3 localization.

Lower levels of ribosomal proteins RpL13 and RpS6 in cells with reduced ns3

S. cerevisiae lsg1 loss-of-function mutants cause retention of the 60S subunit protein RpL25 in nucleoli, indicating that

Lsg1 is required for 60S export. Lsg1 works by facilitating recycling of the export adapter (Kallstrom *et al.* 2003). We examined whether NS3 also functions in 60S subunit export by observing the localization of the 60S subunit protein RpL13 in salivary gland cells where *ns3* had been knocked down with RNAi. We expressed *ns3-dsRNA* with *c061-gal4* (*c061 > ns3-dsRNA*), a driver that is active at variable levels in cells of the salivary glands. This convenient tool enabled the assessment of *ns3-RNAi* knockdown consequence relative to nearby wild-type cells where no *ns3-dsRNA* was expressed. A third transgene, *uas-lamin-gfp*, was included to mark cells expressing *ns3-dsRNA*.

In wild-type cells lacking lamin–GFP and therefore lacking *ns3-dsRNA*, RpL13 was localized in the nucleolus, especially its outer layer, to the nucleoplasm, and to the cytoplasm. In cells with *ns3* knocked down, identified by their lamin–GFP and consequently known to be expressing *ns3-dsRNA*, cytoplasmic RpL13 levels were lower (Figure 5, A–D). To quantify the results, average pixel intensities of cytoplasmic RpL13 were measured and then normalized by dividing RpL13 levels in wild-type cells by that of *ns3-dsRNA*-expressing cells. Cytoplasmic RpL13 levels in wild-type cells were 1.4 ± 0.13 times greater than *ns3-dsRNA* expressing cells. This contrasts with unchanged levels of RpL13 in control salivary gland tissues analyzed in parallel that did not carry *ns3-dsRNA* and produced only lamin–GFP (1.1 ± 0.08, $P = 0.04$, *t*-test) (Figure 5I).

To determine whether the effect of *ns3* knockdown was a general influence on ribosomes beyond its specific effect on RpL13, we examined the localization and levels of RpS6, a component of the 40S subunit. RpS6 was observed in the cytoplasm of both wild-type and *ns3-dsRNA*-expressing cells although, like RpL13, its levels were significantly reduced in cells after *ns3* knockdown (Figures 5, E–H). Wild-type cells had 6.0 ± 1.8 times more RpS6 than neighboring cells expressing *ns3-dsRNA*. This contrasts with control salivary glands that did not express *ns3-dsRNA* (1.7 ± 0.2, $P = 0.005$, *t*-test) (Figure 5I). Reduced cytoplasmic RpL13 and RpS6 after *ns3-dsRNA* is consistent with a role for NS3 in 60S subunit export.

ns3^{G0431} developmental defects are rescued with *ns3-yfp* expression driven by the dopaminergic *th-gal4* driver

Previously, a panel of 15 *gal4* drivers with expression in cell subpopulations were used to express *ns3-yfp* in the *ns3^{G0431}* mutant background and test for rescue of the developmental delay and small-body-size phenotypes (Kaplan *et al.* 2008). From this panel, only the *elav-gal4* (*elav > ns3-yfp*) and *ddc-gal4*-driven *ns3-yfp* (*ddc > ns3-yfp*) rescued the mutant. Given that *elav-gal4* is neuron specific and that *ddc-gal4* is expressed in most larval 5-HT- and DA-positive cells, *ns3* mutation likely affects cells in the intersection of the two drivers' expression patterns: 5-HT and/or DA neurons. Lack of rescue with a *th-gal4* driver led to the earlier conclusion that the 5-HT neurons were most important.

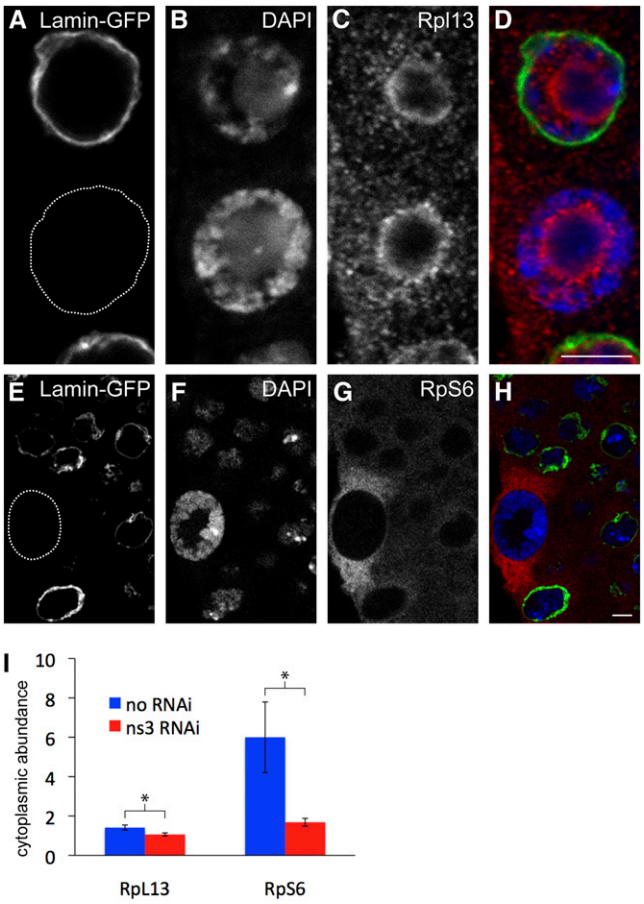

Figure 5 NS3 RNAi reduces the cytoplasmic levels of RpL13 and RpS6 in the salivary glands. (A–D) Anti-RpL13 staining of wild-type and *ns3-dsRNA*-expressing salivary gland cells. The variably active salivary gland driver *c061-gal4* was used to co-express *lamin-gfp* and *ns3-dsRNA*. We observed the consequences for RpL13 localization relative to nearby non-*lamin-gfp*/non-*ns3-dsRNA* expressing cells. (A) Lamin–GFP marks a nucleus from a cell expressing *ns3-dsRNA* and the dotted circle highlights a nucleus from a non-*ns3-dsRNA*-expressing cell. (B) DAPI staining to visualize DNA. (C) Anti-RpL13 staining indicates that RpL13 levels are decreased in the cytoplasm of cells expressing *ns3-dsRNA*. (D) Merged images of A–C. (E–H) Anti-RpS6 staining of *c061 > lamin-gfp, ns3-dsRNA* salivary glands. (E) Lamin–GFP staining indicates *ns3-dsRNA* expressing cells, and the dotted circle highlights a non-*ns3-dsRNA* expressing cell. (F) DAPI to visualize DNA. (G) Anti-RpS6 staining indicates that RpS6 levels are reduced in the cytoplasm of *ns3-dsRNA*-expressing cells. (H) Merged images of E–G. (I) Levels of cytoplasmic RpL13 and RpS6 in non-*lamin-gfp*/non-*ns3-dsRNA* were quantified with imageJ and normalized to neighboring *lamin-gfp/ns3-dsRNA*-expressing cells at the same focal plane. Levels of RpL13 and RpS6 are reduced in the cytoplasm after *ns3* RNAi. Scale bars, 5 μm.

To further define the most highly affected defective neurons in the *ns3^{G0431}* mutant, we tested rescue by *ns3-yfp* expression driven by the newly available *dtrh-gal4* (Alekseyenko *et al.* 2010), which is active in 5-HT neurons. We also retested *th-gal4* for DA neurons (Friggi-Grelin *et al.* 2003). As expected, *ddc > ns3-yfp* provided strong rescue: 76.7 ± 1.4% of *ns3^{G0431}*/Y; *ddc > ns3-yfp* flies eclosed 10 days after embryos were deposited (AEL) (Figure 6A). This contrasts with the negative control *ns3^{G0431}*/Y; *ns3-yfp*/+

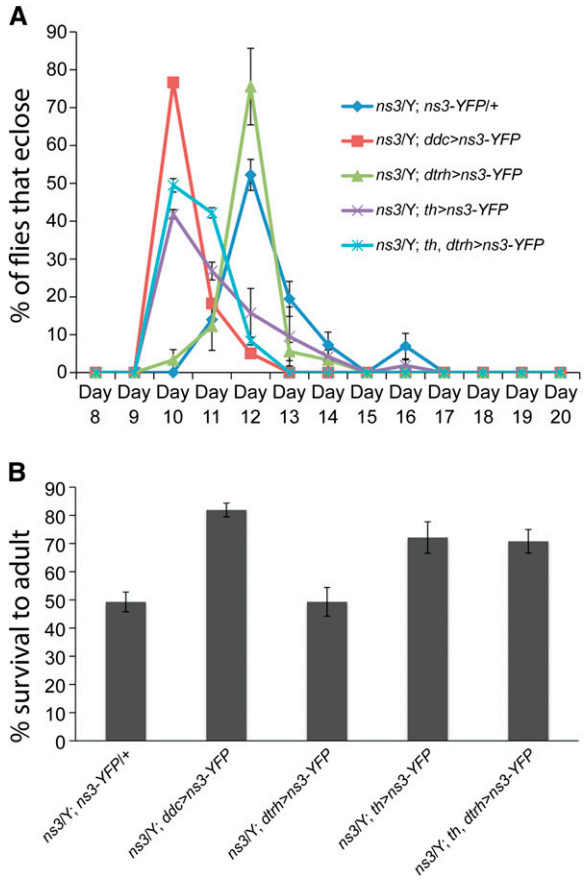

Figure 6 The delayed development and viability of *ns3*^{G0431} mutants can be rescued by restoration of *ns3* function to *th-gal4*-positive cells. (A) Developmental time to eclosion of *ns3*^{G0431}/*Y* males with and without expression of *ns3-yfp* in DA, 5-HT, and DA + 5-HT neurons. Five large crosses were set up of males with (1) no Gal4 driver, (2) DA neuron-enriched *th-gal4*, (3) 5-HT neuron enriched *dtrh-gal4*, (4) DA and 5-HT-enriched *ddc-gal4*, and (5) DA and 5-HT enriched *th-gal4*, *dtrh-gal4* to *ns3*^{G0431}/FM7i, *act* > *gfp*; *uas-ns3-yfp* virgin females. Embryos were collected on yeast/molasses agar plates overnight and aged 24 hr. Forty *act* > *gfp* negative, *ns3*^{G0431}/*Y* male, and *ns3*^{G0431}/+ female larvae were transferred to standard molasses food in vials in triplicate. Eclosion of flies after embryos were laid (AEL) was scored daily, and the plot in A indicates the percentage of the final total number of eclosed *ns3*^{G0431}/*Y* flies that eclosed on the indicated day AEL. Most *ns3*^{G0431}/*Y* flies with no *gal4* driver (dark blue) eclosed 12 days AEL (*N* = 15, 7, and 13 *ns3*^{G0431}/*Y* flies for each of 3 replicates). Expression of *ns3-yfp* in *ns3*^{G0431}/*Y* flies with the *ddc-gal4* (DA + 5-HT, red, *N* = 25, 20, and 16 flies) and *th-gal4* (DA, purple, *N* = 14, 18, and 16 flies) provided substantial rescue, with most flies eclosing 10 days AEL. Expression of *ns3-yfp* with *dtrh-gal4* (5-HT, green, *N* = 10, 7, and 15 flies) did not rescue *ns3*^{G0431}/*Y* developmental delay, and *dtrh-gal4* in combination with *th-gal4* (DA + 5-HT, light blue, *N* = 17, 11, and 20 flies) did not significantly enhance rescue provided by *th-gal4* alone (purple). (B) Survival to adulthood of *ns3*^{G0431}/*Y* males with and without expression of *ns3-yfp* in DA, 5-HT, and DA + 5-HT neurons. The total number of *ns3*^{G0431}/*Y* male flies that eclosed over the predicted number (40 − number of *ns3*^{G0431}/+ females) from three replicates of vials that carried 40 *ns3*^{G0431}/*Y* and *ns3*^{G0431}/+ larvae is plotted. Only 49.3 ± 3.5% of *ns3*^{G0431}/*Y*; *ns3-yfp*/+ and 49.3 ± 5.1% of *ns3*^{G0431}/*Y*; *dtrh* > *ns3-yfp* males survived to adulthood. In contrast, 81.9 ± 2.4% *ns3*^{G0431}/*Y* males carrying *ddc* > *ns3-yfp* and 72.1 ± 5.6% carrying *th* > *ns3-yfp* eclosed. This indicated that expression of *ns3-yfp* in *ns3*^{G0431}/*Y* *ddc/th-gal4*+ cells, covering most DA neurons, restored *ns3*^{G0431}/*Y* viability. Inclusion of the *dtrh-gal4* driver with *th-gal4* did not enhance the rescue provided by *th-gal4* alone, as 70.1 ± 4.2% *ns3*^{G0431}/*Y*; *dtrh*, *th* > *ns3-yfp* males survived.

flies, where no *gal4* driver is present and most flies (52.2 ± 4.1%) eclosed 2 days later on day 12 AEL. Driving NS3–YFP production with *dtrh* > *ns3-yfp* did not rescue, but *ns3*^{G0431}/Y flies with *th* > *ns3-yfp* were substantially rescued: the largest percentage of flies eclosed on day 10 (41.8 ± 1.2%). Adding the 5-HT driver, *dtrh-gal4* to *th-gal4* did not improve the rescue: 49.5 ± 1.8% of the *ns3*^{G0431}/Y; *dtrh*, *th* > *ns3-yfp* flies eclosed on day 10. This trend was matched when looking at viability levels. Only 49.3 ± 3.5% of *ns3*^{G0431}/Y; *ns3-yfp*/+ and 49.3 ± 5.1% of *ns3*^{G0431}/Y; *dtrh* > *ns3-yfp* males survived to adulthood, while 81.9 ± 2.4%, 72.1 ± 5.6%, and 70.1 ± 4.2% of the expected *ns3*^{G0431}/Y males carrying *ddc* > *ns3-yfp*, *th* > *ns3-yfp*, and *dtrh*, *th* > *ns3-yfp* *ns3*^{G0431}/Y survived (Figure 6B).

Given that the cells that activate both *elav-gal4* and *th-gal4* are mostly DA neurons, we suspect that DA neurons are especially prone to defects when NS3 dose is reduced in the hypomorphic *ns3*^{G0431} background. The level of NS3 in *ns3*^{G0431} DA neurons relative to surrounding non-DA neurons was unchanged relative to wild type, ruling out an allele-specific effect on NS3 dosage in DA neurons (Figure S3). The role of NS3 in DA neurons may be to support proper translational regulation of transcripts unique and necessary to DA function, or DA neurons may have an especially high demand for efficient protein synthesis. Although a role of DA in wild-type growth has not been directly observed, the rescue of growth defects of *ns3*^{G0431} with *elav*-, *ddc*-, and *th-gal4*-driven *uas-ns3-yfp* implies that DA neurons provide critical functions for proper larval developmental progression.

Discussion

Evolutionary conservation and possible divergence of Lsg1/NS3 functionality

In yeast, Lsg1p is a cytoplasmic GTPase associated with the 60S ribosomal subunit. It is required for releasing the nuclear export adapter Nmd3p from the 60S ribosomal subunit and therefore indirectly promotes 60S nuclear export (Kallstrom *et al.* 2003; Hedges *et al.* 2005). In this study, we found that expression of fly NS3 in yeast cells was sufficient to rescue Lsg1p deficiency, confirming their orthology. Thus NS3 appears to ensure proper export of the 60S subunit from the nucleus, like Lsg1p. Consistent with this view, levels of RpL13, a large ribosomal protein, were lower in the cytoplasm of salivary gland cells where *ns3* was knocked down with RNAi (Figures 5, A–D and I). Levels of a small ribosomal subunit protein, RpS6, were also reduced after *ns3* knockdown (Figure 5, E–H, 5I). Therefore, NS3 likely contributes to one or more steps that culminate in proper protein synthesis.

We previously showed that expression of a *uas-ns3-yfp* transgene under the control of *ddc-gal4* could strongly rescue the *ns3*^{G0431} mutant. Expression of *uas-lsg1* in this same fashion was not sufficient to provide rescue of the *ns3*^{G0431} mutant (Figures 1, C and D). This apparent contradiction may be explained by features of fly NS3 that suggest functional divergence from yeast Lsg1p. NS3 localizes within or proximal to the nuclear envelope and plasma membrane and is found within cytoplasmic puncta. Lsg1p was not described to be in these subcellular regions and exists throughout the cytoplasm (Kallstrom *et al.* 2003; Hedges *et al.* 2005). The distinctive localization features of NS3 may reflect special features that were acquired in the metazoan lineage, precluding yeast Lsg1p from rescuing the fly *ns3* mutant.

The human protein that is orthologous to Lsg1p/NS3 is hLsg1 (Reynaud *et al.* 2005). Like yeast and fly Lsg1p/NS3, hLsg1 is necessary for cell viability. It is unclear whether hLsg1 has specific roles in ribosome biogenesis, although this is likely given its protein sequence similarity to the yeast ortholog. NS3 and hLsg1 share localization properties. Both proteins are coincident with the nuclear envelope and located in unidentified cytoplasmic puncta (Figure 4J and Figure S1) (Reynaud *et al.* 2005). We did not observe NS3 in the nucleus, yet hLsg1 was observed in nuclear Cajal bodies that contain many factors involved in pre-ribosomal RNA and mRNA processing (Reynaud *et al.* 2005). Just as NS3 and Lsg1p have functional differences, hLsg1 appears to have features and functions different from NS3.

Cell-autonomous role of NS3 revealed by new alleles

In yeast and human cells, Lsg1 is essential for cell viability and growth (Kallstrom *et al.* 2003; Hedges *et al.* 2005; Reynaud *et al.* 2005), yet the *Drosophila ns3*^{G0431} allele was only partially lethal. Many *ns3*^{G0431} flies survive to adulthood, albeit with developmental delay and decreased overall size (Kaplan *et al.* 2008). Here we identified two alleles of the previously uncharacterized locus *l(1)2Ad* as new alleles of *ns3*. Both *ns3*$^{l(1)2Ad1}$ and *ns3*$^{l(1)2Ad3}$, which are predicted to have severe truncation of the protein, cause 100% lethality and are therefore likely strong loss-of-function alleles. In contrast, the *ns3*^{G0431} lesion is a *P*-element insertion in the 5′-UTR, which may cause only a subtle loss-of-function. The apparent inconsistency between cell lethality in *lsg1* mutant yeast and mammalian cells and semiviability in fly cells was resolved by the lethality of the stronger loss-of-function *ns3* alleles. We suspect that most or all *Drosophila* cells depend upon NS3 for ribosome biogenesis and therefore growth and viability. Flies with the *ns3*^{G0431} allele likely survive to adulthood due to a more subtle drop in NS3 levels.

A family of noncanonical GTPases with unified roles in ribosome biogenesis

The canonical GTPase structure, based on Ras, carries G-domain motifs ordered from the N to C terminus as G1–G2–G3–G4–G5. Lsg1 and NS3 contain circularly permuted G-domain motifs that are instead ordered G4–G5–G1–G2–G3 (Figure 3A). This structure is common for GTPases involved in ribosome biogenesis. Several ribosome biogenesis proteins belong to a family of circularly permuted GTPases that expanded in eukarya from a single circularly permuted GTPase, YlqF (Reynaud *et al.* 2005) (Table 1). YlqF itself promotes ribosome biogenesis as it is necessary for 70S assembly in *Bacillus subtilis* (Uicker *et al.* 2006).

In spite of their atypical structures, several circularly permuted GTPases within the YRG family have been demonstrated to be genuine GTPases using crystal structures or *in vitro* assays (Daigle and Brown 2004; Levdikov *et al.* 2004; Shin *et al.* 2004; Reynaud *et al.* 2005; Bassler *et al.* 2006; Cladiere *et al.* 2006; Matsuo *et al.* 2007; Moreau *et al.* 2008; Sudhamsu *et al.* 2008). Altered G-domain ordering does not change how each motif folds into a tertiary structure. Here we demonstrate that NS3 is proficient in GTP hydrolysis and that proper GTPase activity may confer special protein localization properties in neurons, perhaps by affecting association with other proteins.

Based on previous studies of GTPases, replacement of lysine at position 350 in NS3 with asparagine (K350N) is predicted to disrupt the coordination and catalysis of GTP (Saraste *et al.* 1990). We found that production of a protein with this mutation conferred antimorphic activities in flies (Figure 3). This mimics what occurs in *S. cerevisiae* with an analogous mutation (Hedges *et al.* 2005). We suggest that the antimorphic NS3(K350N) blocks important functions, or sequesters essential cofactors away from endogenous wild-type NS3. GTP hydrolysis may be necessary to remove Nmd3 from the 60S subunit and enable its return to the nucleus for another round of 60S export. In this scenario, NS3(K350N) could prevent GTPase-competent wild-type NS3 from removing Nmd3. On the other hand, NS3(K350N) had altered localization in neurons and appeared to spread from cell bodies into neurites. The altered localization could sequester important cofactors away from endogenous NS3 and thus block its ribosome biogenesis activities.

Identifying neuronal subsets involved in growth control

Previously, we had concluded that *ns3* functioned within 5-HT neurons to promote growth (Kaplan *et al.* 2008). The primary data leading to that conclusion were that expression of *uas-ns3-yfp* in most 5-HT and DA neurons (*ddc* > *ns3-yfp*) rescued the *ns3*^{G0431} growth defects, while expression in most DA neurons (*th* > *ns3-yfp)* did not provide rescue. We no longer believe that second, negative, result. Since that study, it has become apparent that the penetrance of *ns3*^{G0431} phenotypes is highly dependent upon genetic background. For instance, the original background of the 5-HT driver line (*dtrh-gal4)* was nearly 100% lethal when placed in *trans* to our *ns3*^{G0431} stock. We therefore backcrossed *ddc-gal4*, *dtrh-gal4*, and *th-gal4* for five generations into an isogenized genetic background (Gohl *et al.* 2011) that we found to be semiviable in *trans* to *ns3*^{G0431}. A second

demonstration of the importance of levels of rescuing protein comes from manipulating the temperature of the experiments and therefore the GAL4 activity level. Our previous studies were performed at 25°. The present studies were conducted at 29°, which significantly boosts expression of Gal4-driven transgenes. Under the conditions of boosted *gal4* expression in pure genetic backgrounds, expression of *uas-ns3-yfp* in DA neurons (*th > ns3-YFP*) provided substantial rescue.

Expression of *ns3* with three different Gal4 drivers (*elav-gal4*, *ddc-gal4*, and *th-gal4*) has been sufficient to provide significant rescue of the $ns3^{G0431}$ mutant. The intersection between these drivers' expression patterns consists of DA neurons, suggesting that *ns3* has an important role in these cells to promote growth. Perhaps factors involved in DA signaling-specific properties have an especially high requirement for protein-translation efficiency. Such growth-promoting properties of DA neurons may include broad-reaching metabolism regulation like that of insulin-like peptides (ILPs), as previously suggested (Kaplan *et al.* 2008). ILPs are produced from a small cluster of neurosecretory cells known as ILP-producing cells (IPCs) (Rulifson *et al.* 2002). ILPs accumulate in IPCs in $ns3^{G0431}$ mutants (Kaplan *et al.* 2008). Perhaps specific signaling defects from DA neurons in the $ns3^{G0431}$ mutant lead to failed ILP modification and/or secretion from IPCs. DA neurons may also regulate nutrient acquisition activities at one or more levels such as appetite control, nutrient absorption, or feeding activities.

5-HT signaling could still be altered in the $ns3^{G0431}$ background. In keeping with that possibility, 5-HT levels were elevated in mutant adult heads. Feeding the 5-HT precursor, 5-HTP, enhanced the $ns3^{G0431}$ phenotypes (Kaplan *et al.* 2008). Those results could be a consequence of the primary defect of *ns3* loss. Recent studies have implicated 5-HT in promoting some activities of IPCs, which in turn are necessary for growth. Developmental growth roles of 5-HT were not demonstrated, yet the expression of the 5-HT1A receptor *gal4* line in IPCs (Luo *et al.* 2012) suggests that 5-HT may regulate IPC-driven growth in certain circumstances.

The $ns3^{G0431}$ mutant appears to be a sensitized genetic condition, where important growth control by *ddc-gal4* and *th-gal4* (*ddc/th-gal4*)-expressing cells is revealed. Alternatively, growth control via *ddc/th-gal4* cells may not happen in wild-type animals, while in $ns3^{G0431}$ mutants an abnormal circuit of this sort occurs. If some aspect of neuronal signaling is subfunctional in the $ns3^{G0431}$ mutant, then restoration of *ddc/th-gal4* cellular health through expression of *uas-ns3-yfp* could compensate for neuronal defects elsewhere. Although *ddc/th-gal4*-expressing cells may convey growth-promoting activities in wild-type flies, these may be DA independent. Both of these drivers are active in a small number of non-dopaminergic neurons and in various other tissues that may be the true source of nonautonomous growth control. In addition, *ddc/th-gal4* growth control may be neuronal, yet mediated by a signaling molecule other than DA such as a neuropeptide, hormone, or different neurotransmitter.

A higher demand for NS3 in neurons

Strong alleles of *ns3* reveal cell-autonomous growth roles (Figures 1–5), while the weak $ns3^{G0431}$ allele reveals that *ddc/th-gal4*-expressing neurons (possibly DA neurons) are sensitive to reduced levels of NS3. Based on high sequence homology, it is likely that NS3 promotes ribosome biogenesis. Thus, the hypomorphic $ns3^{G0431}$ allele may indicate special ribosome biogenesis requirements of *ddc/th-gal4*-expressing neurons and/or unique dependency on specific types of translational regulation.

We propose the following alternative working models to explain *ddc/th-gal4* hypersensitivity to NS3 dosage. As the NS3 yeast ortholog (Lsg1) promotes export of 60S subunits from nuclei, NS3 in metazoans may have become necessary for positioning ribosomes within the specialized structures of neurons. Most ribosomal subunits appear in the neuronal cell body, but in several instances ribosomes are localized within axons and dendrites (Craig and Banker 1994; Brittis *et al.* 2002; Kiebler and Bassell 2006; Rolls *et al.* 2007). This subcellular targeting of ribosomes, causing them to move across long distances, may require specialization of ribosome biogenesis proteins like NS3.

NS3 may instead translationally regulate specific mRNA subsets. Given that DA neurons appear to be especially sensitive to NS3 dose, perhaps one or more mRNAs that code for DA synthesis, degradation, transport, or synaptic dynamics is translationally regulated by NS3. A mRNA-specific translational regulation function would make NS3 analogous to mouse *RpL38*. This large subunit ribosomal protein binds specifically to a subset of Hox gene mRNAs and controls their association with the 80S ribosome. Mice carrying a mutant copy of *RpL38* have specific homeotic transformations due to failed translation of these Hox mRNAs (Kondrashov *et al.* 2011).

Another unique translational regulation role that NS3 may play is in the proper localization and translational regulation of certain mRNAs to the synapse. Localized translation is not unique to neurons, yet several RNA-binding proteins that transport, tether, activate, and/or repress translation have been identified in screens for molecules involved in neuronal activities (Costa-Mattioli *et al.* 2009). Perhaps NS3 is necessary for localized translational regulation in neurons by binding certain mRNAs or transporting ribosomal subunits to the relevant site. Further explorations of ribosome biogenesis, and the diversity of ribosomal structures and activities, is likely to reveal specific developmental and physiological functions carried out by presumed "housekeeping" proteins.

Acknowledgments

We thank Michael Dellinger for critiquing the manuscript. We are grateful to Kevin Cook and the Bloomington *Drosophila* Stock Center for help identifying stocks carrying putative *ns3* alleles. We thank Kathleen Beckingham, Sangbin

Park, Seung Kim, Wendy Neckameyer, Jay Hirsh, Eric Rulifson, Ron Alfa, and members of Tom Clandinin's laboratory for helpful discussions. The research was supported by National Institutes of Health grant GM53655 to A.J. and by the Howard Hughes Medical Institute. T.H. is a Robert Black fellow of the Damon Runyon Cancer Research Foundation (DRG-2045-10). J.N. is a postdoctoral fellow, and M.P.S. an Investigator, of the Howard Hughes Medical Institute.

Literature Cited

Alekseyenko, O. V., C. Lee, and E. A. Kravitz, 2010 Targeted manipulation of serotonergic neurotransmission affects the escalation of aggression in adult male *Drosophila melanogaster*. PLoS ONE 5: e10806.

Barrientos, A., D. Korr, K. J. Barwell, C. Sjulsen, C. D. Gajewski *et al.*, 2003 MTG1 codes for a conserved protein required for mitochondrial translation. Mol. Biol. Cell 14: 2292–2302.

Bassler, J., P. Grandi, O. Gadal, T. Lessmann, E. Petfalski *et al.*, 2001 Identification of a 60S preribosomal particle that is closely linked to nuclear export. Mol. Cell 8: 517–529.

Bassler, J., M. Kallas, and E. Hurt, 2006 The NUG1 GTPase reveals and N-terminal RNA-binding domain that is essential for association with 60 S pre-ribosomal particles. J. Biol. Chem. 281: 24737–24744.

Bernards, A., and J. Settleman, 2004 GAP control: regulating the regulators of small GTPases. Trends Cell Biol. 14: 377–385.

Boddapati, N., K. Anbarasu, R. Suryaraja, A. V. Tendulkar, and S. Mahalingam, 2012 Subcellular distribution of the human putative nucleolar GTPase GNL1 is regulated by a novel arginine/lysine-rich domain and a GTP binding domain in a cell cycle-dependent manner. J. Mol. Biol. 416: 346–366.

Bridges, C. B., and T. H. Morgan, 1923 *The Third Chromosome Group of Mutant Characters of Drosophila melanogaster*. Carnegie Institution, Washington, DC.

Brittis, P. A., Q. Lu, and J. G. Flanagan, 2002 Axonal protein synthesis provides a mechanism for localized regulation at an intermediate target. Cell 110: 223–235.

Cladiere, L., K. Hamze, E. Madec, V. M. Levdikov, A. J. Wilkinson *et al.*, 2006 The GTPase, CpgA(YloQ), a putative translation factor, is implicated in morphogenesis in *Bacillus subtilis*. Mol. Genet. Genomics. 275: 409–420.

Costa-Mattioli, M., W. S. Sossin, E. Klann, and N. Sonenberg, 2009 Translational control of long-lasting synaptic plasticity and memory. Neuron 61: 10–26.

Craig, A. M., and G. Banker, 1994 Neuronal polarity. Annu. Rev. Neurosci. 17: 267–310.

Daigle, D. M., and E. D. Brown, 2004 Studies of the interaction of *Escherichia coli* YjeQ with the ribosome in vitro. J. Bacteriol. 186: 1381–1387.

Daigle, D. M., L. Rossi, A. M. Berghuis, L. Aravind, E. V. Koonin *et al.*, 2002 YjeQ, an essential, conserved, uncharacterized protein from *Escherichia coli*, is an unusual GTPase with circularly permuted G-motifs and marked burst kinetics. Biochemistry 41: 11109–11117.

Du, X., M. R. Rao, X. Q. Chen, W. Wu, S. Mahalingam *et al.*, 2006 The homologous putative GTPases Grn1p from fission yeast and the human GNL3L are required for growth and play a role in processing of nucleolar pre-rRNA. Mol. Biol. Cell 17: 460–474.

Friggi-Grelin, F., H. Coulom, M. Meller, D. Gomez, J. Hirsh *et al.*, 2003 Targeted gene expression in Drosophila dopaminergic cells using regulatory sequences from tyrosine hydroxylase. J. Neurobiol. 54: 618–627.

Gadal, O., D. Strauss, J. Kessl, B. Trumpower, D. Tollervey *et al.*, 2001 Nuclear export of 60s ribosomal subunits depends on Xpo1p and requires a nuclear export sequence-containing factor, Nmd3p, that associates with the large subunit protein Rpl10p. Mol. Cell. Biol. 21: 3405–3415.

Gohl, D. M., M. A. Silies, X. J. Gao, S. Bhalerao, F. J. Luongo *et al.*, 2011 A versatile in vivo system for directed dissection of gene expression patterns. Nat. Methods 8: 231–237.

Hedges, J., M. West, and A. W. Johnson, 2005 Release of the export adapter, Nmd3p, from the 60S ribosomal subunit requires Rpl10p and the cytoplasmic GTPase Lsg1p. EMBO J. 24: 567–579.

Henras, A. K., J. Soudet, M. Gerus, S. Lebaron, M. Caizergues-Ferrer *et al.*, 2008 The post-transcriptional steps of eukaryotic ribosome biogenesis. Cellular and molecular life sciences. Cell. Mol. Life Sci. 65: 2334–2359.

Himeno, H., K. Hanawa-Suetsugu, T. Kimura, K. Takagi, W. Sugiyama *et al.*, 2004 A novel GTPase activated by the small subunit of ribosome. Nucleic Acids Res. 32: 5303–5309.

Ho, J. H., G. Kallstrom, and A. W. Johnson, 2000 Nmd3p is a Crm1p-dependent adapter protein for nuclear export of the large ribosomal subunit. J. Cell Biol. 151: 1057–1066.

Hurt, E., S. Hannus, B. Schmelzl, D. Lau, D. Tollervey *et al.*, 1999 A novel in vivo assay reveals inhibition of ribosomal nuclear export in ran-cycle and nucleoporin mutants. J. Cell Biol. 144: 389–401.

Kallstrom, G., J. Hedges, and A. Johnson, 2003 The putative GTPases Nog1p and Lsg1p are required for 60S ribosomal subunit biogenesis and are localized to the nucleus and cytoplasm, respectively. Mol. Cell. Biol. 23: 4344–4355.

Kaplan, D. D., G. Zimmermann, K. Suyama, T. Meyer, and M. P. Scott, 2008 A nucleostemin family GTPase, NS3, acts in serotonergic neurons to regulate insulin signaling and control body size. Genes Dev. 22: 1877–1893.

Kaziro, Y., H. Itoh, T. Kozasa, M. Nakafuku, and T. Satoh, 1991 Structure and function of signal-transducing GTP-binding proteins. Annu. Rev. Biochem. 60: 349–400.

Kiebler, M. A., and G. J. Bassell, 2006 Neuronal RNA granules: movers and makers. Neuron 51: 685–690.

Kondrashov, N., A. Pusic, C. R. Stumpf, K. Shimizu, A. C. Hsieh *et al.*, 2011 Ribosome-mediated specificity in Hox mRNA translation and vertebrate tissue patterning. Cell 145: 383–397.

Lambertsson, A., 1998 The minute genes in Drosophila and their molecular functions. Adv. Genet. 38: 69–134.

Larkin, M. A., G. Blackshields, N. P. Brown, R. Chenna, P. A. McGettigan *et al.*, 2007 Clustal W and Clustal X version 2.0. Bioinformatics 23: 2947–2948.

Leipe, D. D., Y. I. Wolf, E. V. Koonin, and L. Aravind, 2002 Classification and evolution of P-loop GTPases and related ATPases. J. Mol. Biol. 317: 41–72.

Levdikov, V. M., E. V. Blagova, J. A. Brannigan, L. Cladiere, A. A. Antson *et al.*, 2004 The crystal structure of YloQ, a circularly permuted GTPase essential for *Bacillus subtilis* viability. J. Mol. Biol. 340: 767–782.

Li, H., S. Chaney, I. J. Roberts, M. Forte, and J. Hirsh, 2000 Ectopic G-protein expression in dopamine and serotonin neurons blocks cocaine sensitization in *Drosophila melanogaster*. Curr. Biol. 10: 211–214.

Lin, J. I., N. C. Mitchell, M. Kalcina, E. Tchoubrieva, M. J. Stewart *et al.*, 2011 Drosophila ribosomal protein mutants control tissue growth non-autonomously via effects on the prothoracic gland and ecdysone. PLoS Genet. 7: e1002408.

Lo, K. Y., Z. Li, C. Bussiere, S. Bresson, E. M. Marcotte *et al.*, 2010 Defining the pathway of cytoplasmic maturation of the 60S ribosomal subunit. Mol. Cell 39: 196–208.

Luo, J., J. Becnel, C. D. Nichols, and D. R. Nassel, 2012 Insulin-producing cells in the brain of adult Drosophila are regulated by

the serotonin 5–HT1A receptor: cellular and molecular life sciences. Cell. Mol. Life Sci. 69: 471–484.

Marygold, S. J., J. Roote, G. Reuter, A. Lambertsson, M. Ashburner *et al.*, 2007 The ribosomal protein genes and Minute loci of *Drosophila melanogaster*. Genome Biol. 8: R216.

Matsuo, Y., T. Oshima, P. C. Loh, T. Morimoto, and N. Ogasawara, 2007 Isolation and characterization of a dominant negative mutant of *Bacillus subtilis* GTP-binding protein, YlqF, essential for biogenesis and maintenance of the 50 S ribosomal subunit. J. Biol. Chem. 282: 25270–25277.

Matsuo, E., T. Nagamine, S. Matsumoto, and K. Tsuneizumi, 2011 Drosophila GTPase nucleostemin 2 changes cellular distribution during larval development and the GTP-binding motif is essential to nucleoplasmic localization. Biosci. Biotechnol. Biochem. 75: 1511–1515.

Moreau, M., G. I. Lee, Y. Wang, B. R. Crane, and D. F. Klessig, 2008 AtNOS/AtNOA1 is a functional *Arabidopsis thaliana* cGTPase and not a nitric-oxide synthase. J. Biol. Chem. 283: 32957–32967.

Moy, T. I., and P. A. Silver, 1999 Nuclear export of the small ribosomal subunit requires the ran-GTPase cycle and certain nucleoporins. Genes Dev. 13: 2118–2133.

Pai, E. F., U. Krengel, G. A. Petsko, R. S. Goody, W. Kabsch *et al.*, 1990 Refined crystal structure of the triphosphate conformation of H-ras p21 at 1.35 A resolution: implications for the mechanism of GTP hydrolysis. EMBO J. 9: 2351–2359.

Panse, V. G., and A. W. Johnson, 2010 Maturation of eukaryotic ribosomes: acquisition of functionality. Trends Biochem. Sci. 35: 260–266.

Perrimon, N., L. Engstrom, and A. P. Mahowald, 1989 Zygotic lethals with specific maternal effect phenotypes in *Drosophila melanogaster*. I. Loci on the X chromosome. Genetics 121: 333–352.

Reynaud, E. G., M. A. Andrade, F. Bonneau, T. B. Ly, M. Knop *et al.*, 2005 Human Lsg1 defines a family of essential GTPases that correlates with the evolution of compartmentalization. BMC Biol. 3: 21.

Rolls, M. M., D. Satoh, P. J. Clyne, A. L. Henner, T. Uemura *et al.*, 2007 Polarity and intracellular compartmentalization of Drosophila neurons. Neural Dev. 2: 7.

Rosby, R., Z. Cui, E. Rogers, M. A. deLivron, V. L. Robinson *et al.*, 2009 Knockdown of the Drosophila GTPase nucleostemin 1 impairs large ribosomal subunit biogenesis, cell growth, and midgut precursor cell maintenance. Mol. Biol. Cell 20: 4424–4434.

Rulifson, E. J., S. K. Kim, and R. Nusse, 2002 Ablation of insulin-producing neurons in flies: growth and diabetic phenotypes. Science 296: 1118–1120.

Saraste, M., P. R. Sibbald, and A. Wittinghofer, 1990 The P-loop–a common motif in ATP- and GTP-binding proteins. Trends Biochem. Sci. 15: 430–434.

Saveanu, C., D. Bienvenu, A. Namane, P. E. Gleizes, N. Gas *et al.*, 2001 Nog2p, a putative GTPase associated with pre-60S subunits and required for late 60S maturation steps. EMBO J. 20: 6475–6484.

Schneider, C. A., W. S. Rasband, and K. W. Eliceiri, 2012 NIH Image to ImageJ: 25 years of image analysis. Nat. Methods 9: 671–675.

Seiser, R. M., A. E. Sundberg, B. J. Wollam, P. Zobel-Thropp, K. Baldwin *et al.*, 2006 Ltv1 is required for efficient nuclear export of the ribosomal small subunit in *Saccharomyces cerevisiae*. Genetics 174: 679–691.

Shin, D. H., Y. Lou, J. Jancarik, H. Yokota, R. Kim *et al.*, 2004 Crystal structure of YjeQ from *Thermotoga maritima* contains a circularly permuted GTPase domain. Proc. Natl. Acad. Sci. USA 101: 13198–13203.

Sigal, I. S., J. B. Gibbs, J. S. D'Alonzo, G. L. Temeles, B. S. Wolanski *et al.*, 1986 Mutant ras-encoded proteins with altered nucleotide binding exert dominant biological effects. Proc. Natl. Acad. Sci. USA 83: 952–956.

Stage-Zimmermann, T., U. Schmidt, and P. A. Silver, 2000 Factors affecting nuclear export of the 60S ribosomal subunit in vivo. Mol. Biol. Cell 11: 3777–3789.

Staley, J. P., and J. L. Woolford Jr., 2009 Assembly of ribosomes and spliceosomes: complex ribonucleoprotein machines. Curr. Opin. Cell Biol. 21: 109–118.

Strunk, B. S., and K. Karbstein, 2009 Powering through ribosome assembly. RNA 15: 2083–2104.

Sudhamsu, J., G. I. Lee, D. F. Klessig, and B. R. Crane, 2008 The structure of YqeH: an AtNOS1/AtNOA1 ortholog that couples GTP hydrolysis to molecular recognition. J. Biol. Chem. 283: 32968–32976.

Tsai, R. Y., and R. D. McKay, 2002 A nucleolar mechanism controlling cell proliferation in stem cells and cancer cells. Genes Dev. 16: 2991–3003.

Uicker, W. C., L. Schaefer, and R. A. Britton, 2006 The essential GTPase RbgA (YlqF) is required for 50S ribosome assembly in *Bacillus subtilis*. Mol. Microbiol. 59: 528–540.

Wu, J. S., and L. Luo, 2006 A protocol for dissecting *Drosophila melanogaster* brains for live imaging or immunostaining. Nat. Protoc. 1: 2110–2115.

Xue, S., and M. Barna, 2012 Specialized ribosomes: a new frontier in gene regulation and organismal biology. Nat. Rev. Mol. Cell Biol. 13: 355–369.

Yasumoto, H., L. Meng, T. Lin, Q. Zhu, and R. Y. Tsai, 2007 GNL3L inhibits activity of estrogen-related receptor gamma by competing for coactivator binding. J. Cell Sci. 120: 2532–2543.

Zemp, I., and U. Kutay, 2007 Nuclear export and cytoplasmic maturation of ribosomal subunits. FEBS Lett. 581: 2783–2793.

Zhu, Q., L. Meng, J. K. Hsu, T. Lin, J. Teishima *et al.*, 2009 GNL3L stabilizes the TRF1 complex and promotes mitotic transition. J. Cell Biol. 185: 827–839.

Communicating editor: P. K. Geyer

GENETICS

Supporting Information
http://www.genetics.org/lookup/suppl/doi:10.1534/genetics.112.149104/-/DC1

Regulation of Ribosome Biogenesis by Nucleostemin 3 Promotes Local and Systemic Growth in *Drosophila*

Tom A. Hartl, Julie Ni, Jian Cao, Kaye L. Suyama, Stephanie Patchett, Cyril Bussiere, Dan Yi Gui, Sheng Tang, Daniel D. Kaplan, Matthew Fish, Arlen W. Johnson, and Matthew P. Scott

DOI: 10.1534/genetics.112.149104

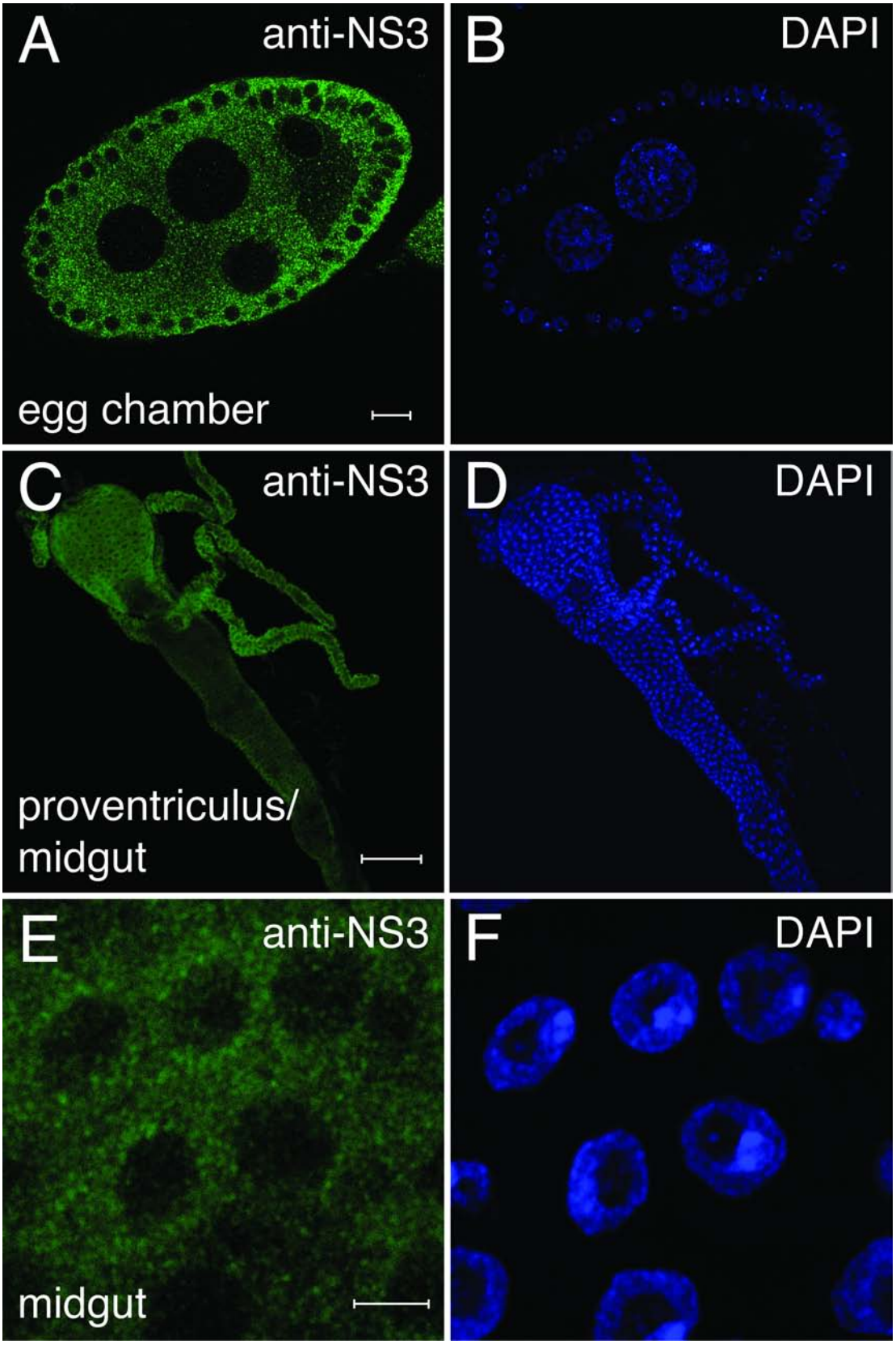

Figure S1 NS3 localization in the ovary/egg chamber, proventriculus, and midgut. A, B. NS3 staining in an egg chamber (stage 8) from a wild-type female demonstrating cytoplasmic enrichment and localization to the periphery of the germinal vesicle. Image captured with a 40X objective at 2X optical zoom. Scale bar in A represents 10µm. **C, D**. NS3 staining in the proventriculus and midgut of a second-instar wild-type larva. NS3 protein is more abundant in the proventriculus than the midgut, yet cytoplasmic in both tissues. Image captured with a 20X objective; the scale bar in E indicates 100µm. **E, F.** NS3 protein in the midgut illustrating cytoplasmic localization and perinuclear enrichment. Image captured with a 63X objective and 8X optical zoom. Scale bar in E indicates 5µm. **G.** Western analysis of embryonic protein extract with the NS3 antibody. The 1 min film exposure reveals that the antibody primarily recognizes NS3 (70kDa) and other minor epitopes become apparent upon longer exposures (5 and 30 min).

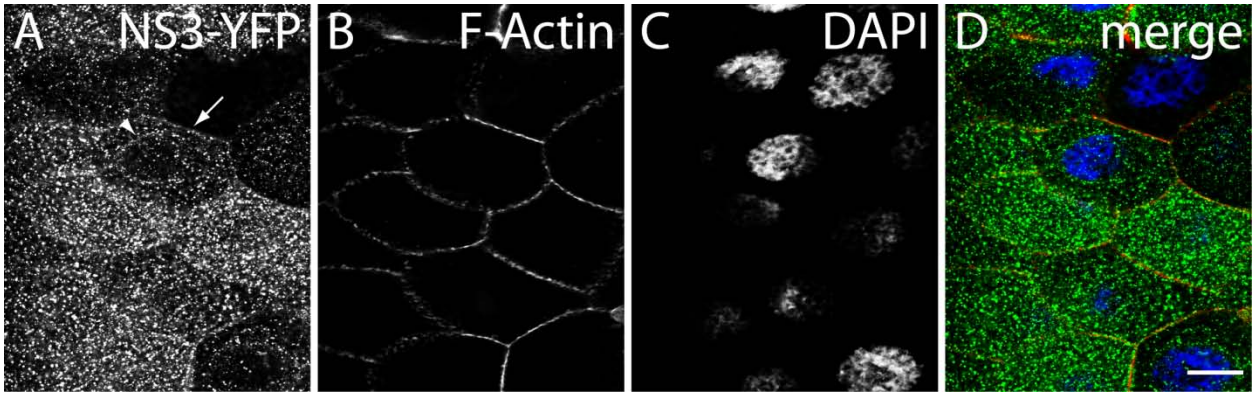

Figure S2 NS3-YFP localizes to cytoplasmic puncta and is enriched proximal to the nuclear envelope and cellular membrane of salivary glands. A-D. NS3-YFP was expressed in salivary glands via *c061-gal4,* a driver that is active at variable levels in cells of the salivary glands. (**A**) NS3-YFP exists within cytoplasmic puncta and is enriched at the nuclear periphery (arrow head) and proximal to the cellular membrane (arrow). (**B**) F-Actin was detected via AlexaFluor conjugated phalloidin to visualize cell exteriors. (**C**) Dapi staining to visualize DNA within the nucleus. (**D**) Merged image of NS3-YFP (green), F-Actin (red), and Dapi (blue) staining. Note the co-localization of NS3-YFP and F-Actin at the cell membrane. Scale bar = 50 µm.

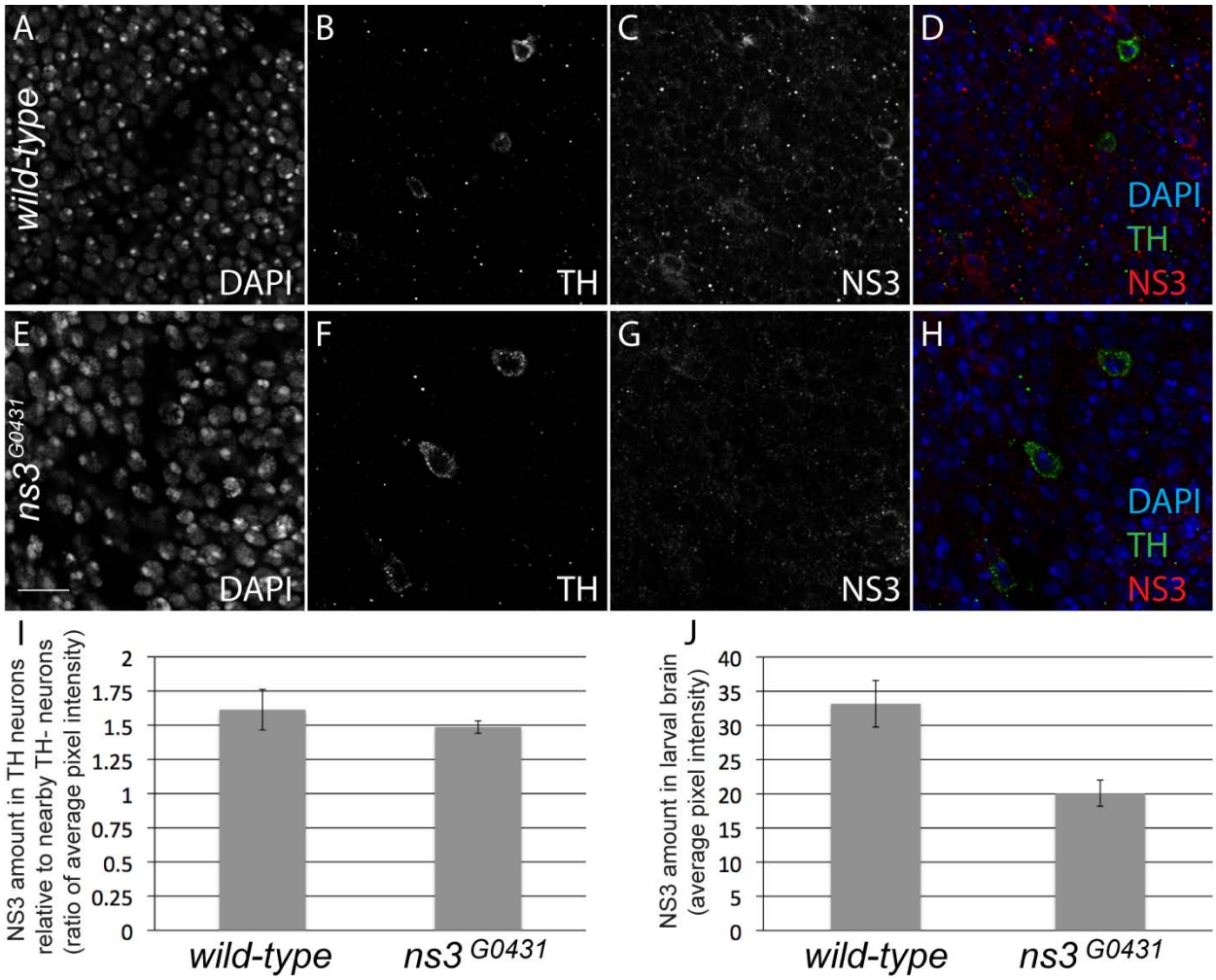

Figure S3 NS3 levels in wild-type and *ns3*^{G0431} mutant larval DA neurons. A-H. The CNS was dissected from wild-type and *ns3*^{G0431} first-instar larvae and stained with anti-tyrosine hydroxylase (TH) and anti-NS3 antibodies. DA neurons were identified by positive staining for TH. Levels of DA neuron NS3 were quantified by manually drawing four lines in the cytoplasm of TH-positive cells, measuring the average pixel intensity of NS3 staining, and averaging the four replicates. These cytoplasmic NS3 values were normalized by dividing by the average pixel intensities of NS3 in surrounding TH-negative cells. TH-negative levels of NS3 were measured by manually drawing five 225 x 225 pixel boxes within TH-negative regions, measuring average pixel intensities of these regions, then taking the mean of all five measurements. **I.** The ratios of TH-positive versus TH-negative NS3 levels, as described above, are plotted for wild-type and *ns3*^{G0431} DA neurons (*N* = 10 DA neurons of each genotype). The levels of NS3 were not changed in DA neurons of *ns3*^{G0431} mutants versus wild-type. **J.** The levels of NS3 in wild-type and *ns3*^{G0431} mutant DA neurons not normalized to surrounding regions. These values served as the normalizing denominator for the data plotted in I. NS3 levels in *ns3*^{G0431} mutants were lower compared to wild-type. However, this trend is not DA neuron-specific and instead represents a general decrease in NS3 levels throughout the CNS. When the DA levels of NS3 were normalized to surrounding regions -- shown in panel I -- there was no decrease in DA neuron NS3 of *ns3*^{G0431} mutants. Thus, NS3 levels throughout the CNS were uniformly decreased throughout the CNS of *ns3*^{G0431} mutants relative to wild-type.